A Robust Optimization Method with Successive Linear Programming for Intensity Modulated Radiation Therapy

Masaaki Tamai [1] and Makoto Yamashita [2]

November 8, 2021.

Abstract: Intensity modulated radiation therapy (IMRT) is one of radiation therapies for cancers, and it is considered to be effective for complicated shapes of tumors, since dose distributions from each irradiation can be modulated arbitrary. Fluence map optimization (FMO), which optimizes beam intensities with given beam angles, is often formulated as an optimization problem with dose volume constraints (DVCs). Romeijn et al. (2003) developed a linear programming (LP) method that approximated DVCs, and Kishimoto and Yamashita (2018) modified it to a successive LP method (SLPM) to find a feasible treatment plan in a wider region than the method of Romeijn et al. However, these two methods did not consider uncertainty, like observational errors or beam inaccuracy, in a series of treatment planning.

In this paper, we propose a numerical method that enhances SLPM utilizing a robust optimization approach. We mathematically prove that the proposed method with extended LP problems holds favorable properties of SLPM, even taking uncertainty in influence matrix into consideration. In particular, when the optimal value of the LP problem is non-positive, the proposed method guarantees that the output solution can satisfy all DVCs. Through numerical experiments, we observed that the proposed method found a feasible plan that SLPM could not find. Even when the proposed method could not output a feasible solution, it was still effective to reduce the largest deviations from DVCs.

Keywords: Intensity modulated radiation therapy, Fluence map optimization, Robust optimization, Linear programming, Conditional Value-at-Risk

1 Introduction

Advances in technology have improved the accuracy and precision of radiation therapy, and radiation therapy is now recognized as one of three major treatments as well as surgery and chemotherapy. Especially, intensity modulated radiation therapy (IMRT) is used to various cases such as concave shapes of tumors, since the radiation irradiated from each beamlet can be modulated to fit the shapes of tumors by controlling the movement of multi leaf collimator (MLC). It is desirable in IMRT treatment planning that tumors (planning target volumes, PTVs) receive a reasonably high dose and healthy organs near tumors (organs at risk, OARs) receive a much low dose [3], and such computation can be formulated as optimization problems.

There are three optimization problems; beam angle optimization (BAO), fluence map optimization (FMO), and leaf sequencing problem. BAO is a problem of minimizing the number of irradiations and optimizing the angle of each irradiation. Minimizing the number of irradiations is to effective ease the burden on the patient, and it is practical to irradiate from 5 to 9 directions [8]. FMO is a problem of optimizing the dose distribution of each irradiation given beam angles. Leaf sequencing problem is a problem of minimizing the movement of MLC under the given dose distribution in order to reduce the treatment time.

[1]Department of Mathematical and Computing Science, Tokyo Institute of Technology, 2-12-1-W8-29 Oookayama, Meguro-ku, Tokyo 152-8552, Japan (tamai.m.ab@m.titech.ac.jp).

[2]Department of Mathematical and Computing Science, Tokyo Institute of Technology, 2-12-1-W8-29 Oookayama, Meguro-ku, Tokyo 152-8552, Japan (Makoto.Yamashita@c.titech.ac.jp). His research was partially supported by JSPS KAKENHI (Grant Number: 21K11767).

FMO frequently contains specific constraints called dose volume constraints (DVCs). However, if we express DVCs rigorously in optimization models, they require integer variables. Solving such optimization problems is known to be NP-hard [18], therefore, a reduction in computation time is an important factor. Romeijn et al. [14, 15] introduced a concept of conditional Value-at-Risk (C-VaR) to replace the DVCs with constraints that can be described in linear programming (LP) problems. Though this C-VaR method reduced the computation time, the region of treatment plan with the C-VaR constraints was much narrower than that with the original DVCs, and this method sometimes failed to find a feasible plan. Kishimoto and Yamashita [12] relaxed the C-VaR constraints by detecting outliers so that the resultant LP problems always have a feasible solution. Their successive LP method (SLPM) repeatedly solved LP problems updating the outliers, and it can find a feasible plan between the C-VaR constraints and the original DVCs.

On the other hand, in medical practice, the sequence of treatment planing includes various uncertainty, such as noises in MRI and CT images, inaccuracy in delivering dose and patient's movements during irradiation. These uncertainty should be addressed to make treatment plans with more robustness. Chan et al. [4, 5] developed an algorithm to reduce an entire error by dividing the set of irradiations into several subsets while updating a lung state for each irradiation based on an assumption that the lung state changes stochastically. Stemkens et al. [17] proposed a framework to generate a subject-specific motion model on a voxel-by-voxel basis by performing a principal component analysis (PCA). However, the C-VaR method and SLPM mentioned did not consider these uncertainty, so these two methods might be vulnerable to such uncertainty.

In this paper, we propose a numerical method that combines a concept of robust optimization with SLPM. It was proved in [12] that SLPM can find a treatment plan that satisfies all the DVCs when the optimal values of its LP problems drop below zero. By extending the proof in [12], we show that the proposed method still possesses this favorable property even though the LP problems in the proposed method involve additional variables for robust optimization.

Through a numerical experiment with test instances of TG119 [10], the proposed method obtains solutions that satisfy all DVCs in more situations than SLPM. Even when the proposed method could not find a feasible solution, we also observe that the proposed method was effective to reduce the largest deviations from DVCs.

In addition, when we extend the objective function in the LP problems with penalty terms, we can give a higher priority to specific DVCs. For the Head and Neck dataset in the TG119 instances, all DVCs are satisfied by the use of the penalty terms, and for the MultiTarget dataset, we can reduce the deviations from the DVCs for the organ that receives the highest doses.

The rest of this paper is organized as follows. In Section 2, we introduce notation related to FMO, then explain existing methods. We describe the proposed method in Section 3, and discuss its mathematical properties. Section 4 shows the results of numerical experiments on the TG119 instances. In Section 5, we discuss an extension of the proposed method by incorporating the uncertainty in lung states considered in Chan et al. [4, 5] and show that a corresponding problem in each iteration remains as an LP problem. Finally, the conclusions are given in Section 6.

2 Preliminaries and Existing Methods

In this section, we briefly introduce notation in FMO, then we describe the C-VaR method by Romeijn et al. [14, 15] that approximates the difficult DVCs by linear constraints. In Section 2.2, we also shortly discuss a framework of the successive LP method (SLPM) in [12].

2.1 DVCs and C-VaR type constraints

In IMRT optimization, to calculate the dose efficiently, the beams are discretized into small areas called beamlets. Similarly, the organs are also discretized into small volumes called voxels. Let $\mathcal{S}$ and $\mathcal{J}$ be the set of organs and the set of beamlets, respectively. We use $\mathcal{I}_s$ to denote the set of voxels in $s \in \mathcal{S}$. We can calculate the dose of the ith voxel in organ $s \in \mathcal{S}$ as $z_{si} = \sum_{j \in \mathcal{J}} [D_s]_{ij} x_j$, where x_j is the inteinsity of beamlet j, and D_s is an influence matrix of organ s, that is, $[D_s]_{ij}$ represents the absorbed dose of voxel i in organ s from beamlet j at unit intensity. The size of D_s is $|\mathcal{I}_s| \times |\mathcal{J}|$, where the notation $|X|$ is used to denote the cardinality of a set X. Through this paper, we use Gray (Gy) as the unit of dose.

For the availability of a treatment plan, it is desirable to satisfy all of dose volume constraints (DVCs). DVCs are classified into two types, lower DVCs and upper DVCs. The lower DVCs are often used for PTVs so that most voxels in PTVs receive doses of a certain level, while the upper DVCs are mainly set for OARs to prevent high irradiation to health tissues. Let $\underline{A}_s \subset (0,1)$ and $\overline{A}_s \subset (0,1)$ denote the sets of ratios used in the lower and upper DVCs for organ s, respectively. A lower (upper) DVC on organ s with respect to a ratio $\alpha \in \underline{A}_s$ ($\alpha \in \overline{A}_s$) is a constraint that the fraction of voxels which receive at least L_s^α Gy should be no less than α (no more than α, respectively). More precisely, a lower DVC and an upper DVC can be formulated as

$$|\{i \in \mathcal{I}_s | z_{si} > L_s^\alpha\}| \geq \alpha |\mathcal{I}_s| \text{ and } |\{i \in \mathcal{I}_s | z_{si} > U_s^\alpha\}| \leq \alpha |\mathcal{I}_s|,$$

respectively. In a mixed-integer linear programming formulation, a lower DVC is composed of the constraints below:

$$z_{si} \geq L_s^\alpha \underline{b}_{si}^\alpha \quad (i \in \mathcal{I}_s), \qquad \sum_{i \in \mathcal{I}_s} \underline{b}_{si}^\alpha \geq \alpha \left|\mathcal{I}_s\right|, \qquad \underline{b}_{si}^\alpha \in \{0,1\} \quad (i \in \mathcal{I}_s)$$

This formulation expresses a DVC rigorously, but it involves a binary variable for each DVC and each voxel, therefore, it often demands long computation time. Acutually, FMO problems with DVCs are proved to be NP-hard [18].

In order to reduce the computation cost, faster optimization approaches that do not involve binary variables are required. Based on a concept of conditional Value-at-Risk (C-VaR) [13], Romeijn et al. [14, 15] replaced the time-consuming lower and upper DVCs with cheaper linear C-VaR constraints of the following forms:

$$\begin{aligned} &\underline{\zeta}_s^\alpha - \frac{1}{(1-\alpha)|\mathcal{I}_s|} \sum_{i \in \mathcal{I}_s} (\underline{\zeta}_s^\alpha - z_{si})^+ \geq L_s^\alpha \quad && s \in \mathcal{S}; \alpha \in \underline{A}_s \\ &\overline{\zeta}_s^\alpha + \frac{1}{\alpha |\mathcal{I}_s|} \sum_{i \in \mathcal{I}_s} (z_{si} - \overline{\zeta}_s^\alpha)^+ \leq U_s^\alpha && s \in \mathcal{S}; \alpha \in \overline{A}_s, \end{aligned} \tag{1}$$

where $\underline{\zeta}_s^\alpha \in \mathbb{R}$ and $\overline{\zeta}_s^\alpha \in \mathbb{R}$ are additional decision variables, and $(x)^+ = \max\{x, 0\}$.

Figure 1 illustrates a difference between a DVC and its C-VaR constraint. (This figure will also be used to illustrate the use of a hot spot in the approach of [12] in the next subsection.) The horizontal axis and the vertical axis represent the absorbed dose (Gy) and the percentage of voxels in a structure, respectively. The blue curve in Figure 1 is a dose volume histogram (DVH); for example, if the histogram passes a point (50 Gy, 95%), 95% of voxels receive a dose of 50 Gy or higher.

For $\alpha \in \overline{A}_s$, a DVC demands that the lowest dose received by the highest α fraction of voxels (the left end of the red and blue areas) be at most U_s^α. In contrast, the C-VaR constraint (1) requires the average dose received by the highest α fraction of voxels (the average of the red and

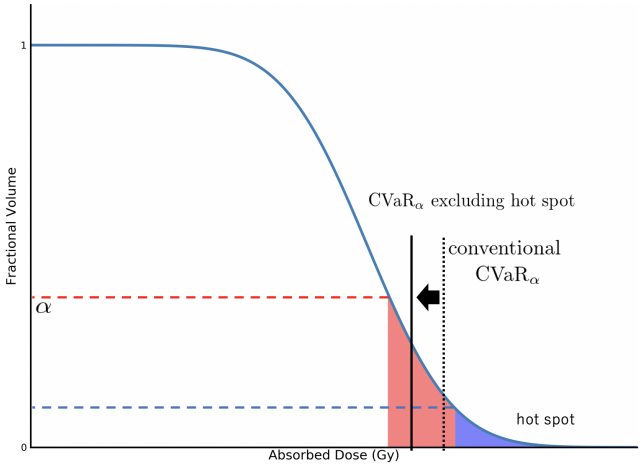

Figure 1: DVH and a comparison between DVC and C-VaR constraint

blue areas, which is indicated by the dotted vertical line "conventional CVaR$_\alpha$") be at most U_s^α. The average dose is larger than the lowest dose, thus any solution satisfying the C-VaR constraint of form (1) also satisfies the original DVC (a mathematical proof of this property was given in [12]). The gap between the average and the lowest doses implies that the feasible region of the C-VaR constraints is narrower than that of the DVCs. Therefore, there is a possibility that the C-VaR method [14, 15] may discard a feasible solution of the original DVCs.

2.2 Successive Linear Programming Method

To reduce the gap between a DVC and the corresponding C-VaR constraint, Kishimoto and Yamashita [12] proposed a successive linear programming method (SLPM) by introducing a concept of hot and cold spots.

The average dose related to an upper DVC is affected strongly by a small number of voxels that receive extremely high doses. In SLPM, such voxels are automatically detected as a hot spot. In Figure 1, a hot spot is illustrated as the blue area. Removing the hot spot from the computation of the average dose shifts the average to the left, thus the gap between the lowest dose and the average dose (in only the red area) will be tighter, therefore, it becomes easier to satisfy the DVC.

A framework of SLPM can be given as Algorithm 1. For the kth iteration, we use $\underline{R}_{k,s}^\alpha \subset \mathcal{I}_s$ and $\overline{R}_{k,s}^\alpha \subset \mathcal{I}_s$ to denote the cold spot and hot spot, respectively, and we solve the following LP:

$$\min\ t \tag{2a}$$

$$\text{s.t.}\quad \sum_{j\in\mathcal{J}} [D_s]_{ij} x_j = z_{si} \qquad s\in\mathcal{S}; i\in\mathcal{I}_s \tag{2b}$$

$$L_s - \underline{P}_s t \le z_{si} \le U_s + \overline{P}_s t \qquad s\in\mathcal{S}; i\in\mathcal{I}_s \tag{2c}$$

$$\underline{\zeta}_s^\alpha - \frac{1}{(1-\alpha)|\mathcal{I}_s| - |\underline{R}_{k,s}^\alpha|} \sum_{i\in\mathcal{I}_s\setminus\underline{R}_{k,s}^\alpha} (\underline{\zeta}_s^\alpha - z_{si})^+ \ge L_s^\alpha - \underline{P}_s^\alpha t \qquad s\in\mathcal{S}; \alpha\in\underline{A}_s \tag{2d}$$

$$\overline{\zeta}_s^\alpha + \frac{1}{\alpha|\mathcal{I}_s| - |\overline{R}_{k,s}^\alpha|} \sum_{i\in\mathcal{I}_s\setminus\overline{R}_{k,s}^\alpha} (z_{si} - \overline{\zeta}_s^\alpha)^+ \le U_s^\alpha + \overline{P}_s^\alpha t \qquad s\in\mathcal{S}; \alpha\in\overline{A}_s \tag{2e}$$

$$x_j,\ z_{si} \ge 0 \qquad s\in\mathcal{S}; i\in\mathcal{I}_s; j\in\mathcal{J} \tag{2f}$$

$$\underline{\zeta}_s^\alpha, \overline{\zeta}_s^\alpha, t \in \mathbb{R} : \text{free variables},$$

In (2), $\underline{P}_s^\alpha, \overline{P}_s^\alpha, \underline{P}_s, \overline{P}_s$ are parameters that control weights of DVCs. The constraint (2c) is derived from bounds $L_s \leq z_{si} \leq U_s$ that each voxel should satisfy. The cold spot $\underline{R}_{k,s}^\alpha$ and the hot spot $\overline{R}_{k,s}^\alpha$ are removed from the computation for the averages in (2d) and (2e), respectively. These spots are updated by the rule (3) in Algorithm 1.

Algorithm 1 A framework of Successive Linear Programming Method

Initialize: Set parameters $\underline{P}_s^\alpha, \overline{P}_s^\alpha, \underline{P}_s, \overline{P}_s$ with positive values, and set maximum number of iterations with K. Let the initial cold and hot spots be empty sets; $\underline{R}_{1,s}^\alpha = \emptyset$ and $\overline{R}_{k,s}^\alpha = \emptyset$.

for $k = 1$ to K **do**
Solve the kth LP problem (2) and let its optimal value be t_k and the optimal beam intensities be x^k.
Calculate absorbed dose $z_{si} = \sum_{j \in \mathcal{J}} [D_s]_{ij} x_j^k$, and update cold and hot spots by the following rules:

$$\underline{R}_{(k+1),s}^\alpha = \left\{ i | z_{si} < L_s^\alpha - \underline{P}_s^\alpha t_k \right\}, \qquad \overline{R}_{(k+1),s}^\alpha = \left\{ i | z_{si} > U_s^\alpha + \overline{P}_s^\alpha t_k \right\} \tag{3}$$

end for
return x^K

Kishimoto and Yamashita [12] proved the following proposition.

Proposition 1. [12] SLPM with (2) as the kth LP problem enjoys the following three properties:

(i) For each $k \geq 1$, the kth LP (2) has an optimal solution.
(ii) If the optimal value t_k in the kth LP (2) satisfies $t_k \leq 0$, then all DVCs are satisfied.
(iii) The sequence $\{t_k\}$ is monotonically non-increasing, that is $t_{k+1} \leq t_k$ for $k \geq 1$.

It was pointed out in [12] that the optimal value t_k in (2) can be regarded as the largest deviation from DVCs at the kth iteration adjusted by the parameters $\underline{P}_s^\alpha, \overline{P}_s^\alpha, \underline{P}_s$, and $\overline{P}_s$. Property (i) guarantees that Algorithm 1 can find a solution in each iteration, since SLPM can detect the cold and hot spots adequately. This is different from the C-VaR method [14, 15], which cannot output useful information if no solution can satisfy all the C-VaR constraints even when there is a solution that satisfies all DVCs. Furthermore, due to Property (iii), SLPM reduces the deviation in each iteration, and this leads to a solution that satisfies all DVCs when $t_k \leq 0$ in Property (ii).

2.3 Robust Optimization

For latter discussions, we give a brief introduction of robust optimization (for more details, see Bental et al. [1] and the references therein). Roughly speaking, the concept of robust optimization is to optimize a given objective function over a feasible set that includes uncertainty. Suppose that we are solving an optimization problem

$$\min \sum_{i=1}^n c_i y_i \quad \text{s.t.} \quad \sum_{i=1}^n a_i y_i \leq b, \tag{4}$$

where the input data are $a \in \mathbb{R}^n, b \in \mathbb{R}, c \in \mathbb{R}^n$. We assume that $(a, b) \in \mathbb{R}^n \times \mathbb{R}$ belongs to an uncertainty set $\mathcal{U} = \left\{ (a,b) \middle| (a,b) = (a^0, b^0) + \sum_{l=1}^L \xi_l (a^l, b^l) : \xi \in \mathcal{Z} \right\}$, where $a_0, a_1, \ldots, a_L \in \mathbb{R}^n$ and $b_0, b_1, \ldots, b_L \in \mathbb{R}$ are parameters and $\mathcal{Z} \subset \mathbb{R}^L$ is a closed convex perturbation set.

In a global robust optimization, the objective function is optimized in a region that the constraints are satisfied for any input data in $\mathcal{Z}$, thus a robust counterpart of (4) can be formulated as

$$\min_{y\in\mathbb{R}^n} \sum_{i=1}^{n} c_i y_i \quad \text{s.t.} \quad \sum_{i=1}^{n} a_i y_i \le b \quad \forall (a,b) \in \mathcal{U}, \tag{5}$$

and this can be equivalently rewritten as

$$\min_{y\in\mathbb{R}^n} \sum_{i=1}^{n} c_i y_i \quad \text{s.t.} \quad \max_{(a,b)\in\mathcal{U}} \left(\sum_{i=1}^{n} a_i y_i - b \right) \le 0. \tag{6}$$

For solving optimization problems that involve constraints like (5) or (6) in a practical time, the perturbation set $\mathcal{Z}$ is usually a box (like $-\delta \le \xi_l \le \delta$ for each $l = 1, \ldots, L$ with a parameter $\delta > 0$) in [16] or an ellipsoid in [1]. It was shown in [1] that optimization problems of a linear objective function over the box or ellipsoid perturbation set can be converted into LP problems or second-order cone programming (SOCP) problems, respectively. Since the computation time is an important factor in the IMRT optimization and the computation cost of LP problems is usually less than that of SOCP problems, our interest is the boxed-shape perturbation set.

3 The Proposed Method

SLPM [12] did not consider data which includes uncertainty of beam irradiations or a movement during treatment, therefore, it is more practical to solve an optimization problem assuming that the data contains uncertainty. We propose a numerical method that combines SLPM with the concept of robust optimization, and we will show that Proposition 1 can still hold in the proposed method.

3.1 The Proposed Method

A framework of the proposed method is given in Algorithm 2 and it is a modification of Algorithm 1 with a replacement of the kth LP problem (2) with its robust counterpart (8) below. We call the proposed method SLPM-R (SLPM with Robust).

Algorithm 2 A framework of the proposed method (SLPM-R)

Initialize: Set parameters $\underline{P}_s^\alpha, \overline{P}_s^\alpha, \underline{P}_s, \overline{P}_s$ with positive values, and set maximum number of iterations with K. Let the initial cold and hot spots be empty sets; $\underline{R}_{1,s}^\alpha = \emptyset$ and $\overline{R}_{k,s}^\alpha = \emptyset$.

for $k = 1$ to K **do**

Solve the kth extended LP problem (8) and let its optimal value be t_k and the optimal beam intensities be x^k.

Calculate absorbed doses $\underline{z}_{si} = \sum_{j\in\mathcal{J}} [D_s - \delta |D_s'|]_{ij} x_j^k$ and $\overline{z}_{si} = \sum_{j\in\mathcal{J}} [D_s + \delta |D_s'|]_{ij} x_j^k$, and update cold and hot spots by the following rules:

$$\underline{R}_{(k+1),s}^\alpha = \left\{ i | \underline{z}_{si} < L_s^\alpha - \underline{P}_s^\alpha t_k \right\}, \qquad \overline{R}_{(k+1),s}^\alpha = \left\{ i | \overline{z}_{si} > U_s^\alpha + \overline{P}_s^\alpha t_k \right\}. \tag{7}$$

end for

return x^K

A treatment plan in clinical practice contains various uncertainty, such as measurement errors in CT and MRI imaging, numerical errors in QIB method [11]. In the proposed method, we focus uncertainty in the influence matrix and assume that other uncertainty elements are implicitly reflected in uncertainty of the influence matrix.

Recall that the order of the influence matrix D_s is $|\mathcal{I}_s| \times |\mathcal{J}|$. We assume that a perturbation set $\mathcal{Z}_s$ is given as a box set, so that D_s is described as

$$D_s = D_s^0 + \Xi_s \circ D_s^{'},$$

where $X \circ Y$ is the element-wise product ($[X \circ Y]_{ij} = X_{ij} \cdot Y_{ij}$), $D_s^0 \in \mathbb{R}^{|\mathcal{I}_s| \times |\mathcal{J}|}$ and $D_s^{'} \in \mathbb{R}^{|\mathcal{I}_s| \times |\mathcal{J}|}$ are parameter matrices and Ξ_s is taken from the box-shaped perturbation set

$$\mathcal{Z}_s = \left\{ \Xi_s \in \mathbb{R}^{|\mathcal{I}_s| \times |\mathcal{J}|} \;\middle|\; -\delta \leq [\Xi_s]_{ij} \leq \delta \quad \text{for} \quad i = 1, \ldots, m,\ j = 1, \ldots, n \right\}.$$

We can choose the same $\delta > 0$ for all voxels by adjusting D_s^0 and $D_s^{'}$ appropriately. For instance, if $3 \leq [D_s]_{11} \leq 7$ and $10 \leq [D_s]_{12} \leq 12$, we take $[D_s^0]_{11} = 5, [D_s^0]_{12} = 11, [D_s^{'}]_{11} = 2, [D_s^{'}]_{12} = 1$ with $\delta = 1$. In the numerical experiment later, we will change δ to evaluate the effect of the uncertainty range.

To derive the robust counterpart of the LP problem (2) in SLPM, we first focus on an upper bound for each voxel of form $\sum_{j \in \mathcal{J}} [D_s]_{ij} x_j \leq U_s + \overline{P}_s t$. In similar steps from (4) to (6), we convert this constraint:

$$\begin{aligned}
\sum_{j \in \mathcal{J}} [D_s]_{ij} x_j \leq U_s + \overline{P}_s t \Rightarrow & \sum_{j \in \mathcal{J}} [D_s^0 + \Xi_s \circ D_s^{'}]_{ij} x_j \leq U_s + \overline{P}_s t \quad \forall \Xi_s \in \mathcal{Z}_s \\
\Leftrightarrow & \sum_{j \in \mathcal{J}} [D_s^0]_{ij} x_j + \max_{\Xi_s \in \mathcal{Z}_s} \sum_{j \in \mathcal{J}} [\Xi_s \circ D_s^{'}]_{ij} x_j \leq U_s + \overline{P}_s t \\
\Leftrightarrow & \sum_{j \in \mathcal{J}} [D_s^0]_{ij} x_j + \delta \sum_{j \in \mathcal{J}} |[D_s^{'}]_{ij}| x_j \leq U_s + \overline{P}_s t \\
\Leftrightarrow & \sum_{j \in \mathcal{J}} [D_s^0 + \delta |D_s^{'}|]_{ij} x_j \leq U_s + \overline{P}_s t,
\end{aligned}$$

where $|D_s^{'}|$ is the matrix who takes element-wise absolute values of $D_s^{'}$.

To apply the same procedure to the inequalities in (2), we split the variable z_{si} into two variables $\underline{z}_{si}$ and $\overline{z}_{si}$ for lower and upper DVCs, respectively. Consequently, we derive the robust

counterpart of (2) as follows:

$$\min\ t \tag{8a}$$

$$\text{s.t.}\quad \sum_{j\in\mathcal{J}}[D_s^0-\delta|D_s'|]_{ij}x_j=\underline{z}_{si} \qquad s\in\mathcal{S};i\in\mathcal{I}_s \tag{8b}$$

$$\sum_{j\in\mathcal{J}}[D_s^0+\delta|[D_s'|]_{ij}x_j=\overline{z}_{si} \qquad s\in\mathcal{S};i\in\mathcal{I}_s \tag{8c}$$

$$L_s-\underline{P}_s t\le \underline{z}_{si} \qquad s\in\mathcal{S};i\in\mathcal{I}_s \tag{8d}$$

$$\overline{z}_{si}\le U_s+\overline{P}_s t \qquad s\in\mathcal{S};i\in\mathcal{I}_s \tag{8e}$$

$$\underline{\zeta}_s^\alpha-\frac{1}{(1-\alpha)|\mathcal{I}_s|-|\underline{R}_{k,s}^\alpha|}\sum_{i\in\mathcal{I}_s\setminus\underline{R}_{k,s}^\alpha}(\underline{\zeta}_s^\alpha-\underline{z}_{si})^+\ge L_s^\alpha-\underline{P}_s^\alpha t \qquad s\in\mathcal{S};\alpha\in\underline{A}_s \tag{8f}$$

$$\overline{\zeta}_s^\alpha+\frac{1}{\alpha|\mathcal{I}_s|-|\overline{R}_{k,s}^\alpha|}\sum_{i\in\mathcal{I}_s\setminus\overline{R}_{k,s}^\alpha}(\overline{z}_{si}-\overline{\zeta}_s^\alpha)^+\le U_s^\alpha+\overline{P}_s^\alpha t \qquad s\in\mathcal{S};\alpha\in\overline{A}_s \tag{8g}$$

$$x_j,\ \underline{z}_{si},\ \overline{z}_{si}\ge 0 \qquad s\in\mathcal{S};i\in\mathcal{I}_s;j\in\mathcal{J} \tag{8h}$$

$$\underline{\zeta}_s^\alpha,\overline{\zeta}_s^\alpha,t:\text{ free variables.}$$

Corresponding to the split of z_{si} into $\underline{z}_{si}$ and $\overline{z}_{si}$, the update rule (3) in SLPM for the cold spots and hot spots are modified as (7) in SLPM-R.

In (8), we use the simple objective function t in the same way as (2). We will consider a variant of this objective function in Section 3.3.

3.2 Properties of The Proposed Method

The proposed method (SLPM-R) shares the basic framework with SLPM of [12]. However, it is not obvious whether SLPM-R can keep the three properties in Proposition 1, since we split z_{si} into $\underline{z}_{si}$ and $\overline{z}_{si}$. Therefore, we extend the proof in [12] along with SLPM-R. As a result, SLPM-R retains the properties and this indicates that SLPM-R can find a favorable treatment plan within robust optimization.

Proposition 2. The three properties (i), (ii) and (iii) in Proposition 1 hold in SLPM-R.

To prove Proposition 2, we will use Lemma 1 below. Thus, we first give a proof for Lemma 1, then prove Proposition 2.

Lemma 1. For each $s\in\mathcal{S}$ and $\alpha\in\underline{A}_s$, any feasible point in (8) satisfies $t\ge\left(\max_{i\in\mathcal{I}_s\setminus\underline{R}_{k,s}^\alpha}\underline{z}_{si}-L_s^\alpha\right)/\underline{P}_s^\alpha$. Similarly, for each $s\in\mathcal{S}$ and $\alpha\in\overline{A}_s$, any feasible point in (8) satisfies $t\ge -U_s^\alpha/\overline{P}_s^\alpha$.

Proof. For each $s\in\mathcal{S},\ \alpha\in\underline{A}_s$, we know $0<\alpha<1$, thus it holds that

$$\begin{aligned}
&\underline{\zeta}_s^\alpha-\frac{1}{(1-\alpha)|\mathcal{I}_s|-|\underline{R}_{k,s}^\alpha|}\sum_{i\in\mathcal{I}_s\setminus\underline{R}_{k,s}^\alpha}(\underline{\zeta}_s^\alpha-\underline{z}_{si})^+\le\underline{\zeta}_s^\alpha-\frac{1}{|\mathcal{I}_s|-|\underline{R}_{k,s}^\alpha|}\sum_{i\in\mathcal{I}_s\setminus\underline{R}_{k,s}^\alpha}(\underline{\zeta}_s^\alpha-\underline{z}_{si})^+\\
=&\frac{1}{|\mathcal{I}_s|-|\underline{R}_{k,s}^\alpha|}\sum_{i\in\mathcal{I}_s\setminus\underline{R}_{k,s}^\alpha}\left\{\underline{\zeta}_s^\alpha-(\underline{\zeta}_s^\alpha-\underline{z}_{si})^+\right\}\le\frac{1}{|\mathcal{I}_s|-|\underline{R}_{k,s}^\alpha|}\sum_{i\in\mathcal{I}_s\setminus\underline{R}_{k,s}^\alpha}\left\{\underline{\zeta}_s^\alpha-(\underline{\zeta}_s^\alpha-\underline{z}_{si})\right\}\\
\le&\frac{1}{|\mathcal{I}_s|-|\underline{R}_{k,s}^\alpha|}\sum_{i\in\mathcal{I}_s\setminus\underline{R}_{k,s}^\alpha}\max_{i\in\mathcal{I}_s\setminus\underline{R}_{k,s}^\alpha}\underline{z}_{si}=\max_{i\in\mathcal{I}_s\setminus\underline{R}_{k,s}^\alpha}\underline{z}_{si}.
\end{aligned}$$

Therefore, from (8f), we obtain $L_s^\alpha - \underline{P}_s^\alpha t \leq \max_{i\in\mathcal{I}_s\setminus\underline{R}_{k,s}^\alpha} \underline{z}_{si}$, and this is equivalent to $t \geq \left(\max_{i\in\mathcal{I}_s\setminus\underline{R}_{k,s}^\alpha} \underline{z}_{si} - L_s^\alpha\right)/\underline{P}_s^\alpha$.

Similarly, for each $s\in\mathcal{S},\ \alpha\in\overline{A}_s$, we know

$$\begin{aligned}
&\overline{\zeta}_s^\alpha + \frac{1}{\alpha|\mathcal{I}_s| - |\overline{R}_{k,s}^\alpha|}\sum_{i\in\mathcal{I}_s\setminus\overline{R}_{k,s}^\alpha}(\overline{z}_{si}-\overline{\zeta}_s^\alpha)^+ \geq \overline{\zeta}_s^\alpha + \frac{1}{|\mathcal{I}_s| - |\overline{R}_{k,s}^\alpha|}\sum_{i\in\mathcal{I}_s\setminus\overline{R}_{k,s}^\alpha}(\overline{z}_{si}-\overline{\zeta}_s^\alpha)^+\\
=&\frac{1}{|\mathcal{I}_s| - |\overline{R}_{k,s}^\alpha|}\sum_{i\in\mathcal{I}_s\setminus\overline{R}_{k,s}^\alpha}\left\{\overline{\zeta}_s^\alpha + (\overline{z}_{si}-\overline{\zeta}_s^\alpha)^+\right\} \geq 0,
\end{aligned}$$

where the last nonnegativity is derived from an inequality $p + (q-p)^+ \geq 0$ which holds for $\forall p\in\mathbb{R}, \forall q\geq 0$. Therefore, from (8g), we obtain $U_s^\alpha + \overline{P}_s^\alpha t \geq 0$. □

We are now prepared to give a proof of Proposition 2.

Proof of Proposition 2. We start from Property (i). Since (8) is an LP problem, we can utilize the duality theorem [6], therefore, it is sufficient to show two points; (a) a feasible solution exists in (8) and (b) there is a lower bound of the objective function t. We will prove these by induction. When $k=1$, it holds for all $s\in\mathcal{S}$ that $(1-\alpha)|\mathcal{I}_s| > |\underline{R}_{1,s}^\alpha|$ and $\alpha|\mathcal{I}_s| > |\overline{R}_{1,s}^\alpha|$, since $\underline{R}_{1,s}^\alpha = \overline{R}_{1,s}^\alpha = \emptyset$ and $0<\alpha<1$, thus the denominators (8f) and (8g) are nonzeros. Let $x_j = 0\ (j\in\mathcal{J}),\ \overline{z}_{si} = \underline{z}_{si} = 0\ (s\in\mathcal{S}, i\in\mathcal{I}_s),\ \overline{\zeta}_s^\alpha = 0\ (s\in\mathcal{S}, \alpha\in\overline{A}_s),\ \underline{\zeta}_s^\alpha = 0\ (s\in\mathcal{S},\ \alpha\in\underline{A}_s)$. By taking t such that $t \geq \max\left\{\frac{L_s}{\underline{P}_s},\ \max_{\alpha\in\underline{A}_s}\left\{\frac{L_s^\alpha}{\underline{P}_s^\alpha}\right\}\right\}$, the LP (8) has at least one feasible solution. Next, we verify a lower bound of the objective function t. From Lemma 1, the objective function t of LP (8) has a lower bound:

$$\begin{aligned}
t \geq&\ \max_{s\in\mathcal{S}}\left\{-\frac{U_s}{\overline{P}_s},\ \frac{L_s - \max_{i\in\mathcal{I}_s}\underline{z}_{si}}{\underline{P}_s},\ \max_{\alpha\in\overline{A}_s}\left\{-\frac{U_s^\alpha}{\overline{P}_s^\alpha}\right\},\ \max_{\alpha\in\underline{A}_s}\left\{\frac{L_s^\alpha - \max_{i\in\mathcal{I}_s}\underline{z}_{si}}{\underline{P}_s^\alpha}\right\}\right\}\\
\geq&\ \max_{s\in\mathcal{S}}\left\{-\frac{U_s}{\overline{P}_s},\ \max_{\alpha\in\overline{A}_s}\left\{-\frac{U_s^\alpha}{\overline{P}_s^\alpha}\right\}\right\}.
\end{aligned}$$

We assume (a) and (b) for the kth LP and consider the $(k+1)$th LP. Let $t_k, x_j^k, \underline{z}_{si}^k, \overline{z}_{si}^k, (\underline{\zeta}_s^\alpha)^k, (\overline{\zeta}_s^\alpha)^k$ denote an optimal solution of the kth LP. For (8g), we suppose temporarily the number of voxels that are newly added to the hot spots after the kth iteration were greater than or equal to $\alpha|\mathcal{I}_s| - |\overline{R}_{k,s}^\alpha|$, that is, $\left|\left\{\overline{z}_{si}^k \middle| \overline{z}_{si}^k > U_s^\alpha + \overline{P}_s^\alpha t_k, \overline{z}_{si}^k \notin \overline{R}_{k,s}^\alpha\right\}\right| \geq \alpha|\mathcal{I}_s| - |\overline{R}_{k,s}^\alpha|$. Then, we have

$$\begin{aligned}
&(\overline{\zeta}_s^\alpha)^k + \frac{1}{\alpha|\mathcal{I}_s| - |\overline{R}_{k,s}^\alpha|}\sum_{i\in\mathcal{I}_s\setminus\overline{R}_{k,s}^\alpha}(\overline{z}_{si}^k - (\overline{\zeta}_s^\alpha)^k)^+\\
>&\ (\overline{\zeta}_s^\alpha)^k + \frac{1}{\alpha|\mathcal{I}_s| - |\overline{R}_{k,s}^\alpha|}(|\mathcal{I}_s| - |\overline{R}_{k,s}^\alpha|)(U_s^\alpha + \overline{P}_s^\alpha t_k - (\overline{\zeta}_s^\alpha)^k)\\
>&\ (\overline{\zeta}_s^\alpha)^k + \frac{1}{\alpha|\mathcal{I}_s| - |\overline{R}_{k,s}^\alpha|}(\alpha|\mathcal{I}_s| - |\overline{R}_{k,s}^\alpha|)(U_s^\alpha + \overline{P}_s^\alpha t_k - (\overline{\zeta}_s^\alpha)^k) = U_s^\alpha + \overline{P}_s^\alpha t_k,
\end{aligned}$$

but this inequality is inconsistent with (8g). Thus, we know that $\left|\left\{\overline{z}_{si}^k \middle| \overline{z}_{si}^k > U_s^\alpha + \overline{P}_s^\alpha t^k, \overline{z}_{si}^k \notin \overline{R}_{k,s}^\alpha\right\}\right|$ is bounded above by $\alpha|\mathcal{I}_s| - |\overline{R}_{k,s}^\alpha|$. Therefore, it holds

$$|\overline{R}_{k+1,s}^\alpha| < (\alpha|\mathcal{I}_s| - |\overline{R}_{k,s}^\alpha|) + |\overline{R}_{k,s}^\alpha| = \alpha|\mathcal{I}_s|. \tag{9}$$

Regarding cold spots, we can also derive $|\underline{R}^{\alpha}_{(k+1),s}| < (1-\alpha)|\mathcal{I}_s|$. Thus, the denominators (8f) and (8g) are nonzeros, and we can apply the same proof as the first iteration to show (a) and (b) in the $(k+1)$th LP.

Next, we consider Property (ii). Recall t_k is the optimal value t of the kth LP (8). When $t_k \leq 0$, $\overline{R}^{\alpha}_{(k+1),s} = \{i|\overline{z}^k_{si} > U^{\alpha}_s + \overline{P}^{\alpha}_s t_k\}$ indicates $\{i|\overline{z}^k_{si} > U^{\alpha}_s\} \subset \overline{R}^{\alpha}_{(k+1),s}$. From (9), we know $\left|\{i|\overline{z}^k_{si} > U^{\alpha}_s\}\right| < \alpha\,|\mathcal{I}_s|$. Due to $-\delta \leq [\Xi_s]_{ij} \leq \delta$ and $x^k_j \geq 0$, we obtain $\sum_{j\in\mathcal{J}}[D^0_s + \Xi_s \circ D^{'}_s]_{ij}x^k_j \leq \sum_{j\in\mathcal{J}}[D^0_s + \delta|D^{'}_s|]_{ij}x^k_j = \overline{z}^k_{si}$, therefore, $\left|\left\{i\middle|\sum_{j\in\mathcal{J}}[D^0_s + \Xi_s \circ D^{'}_s]_{ij}x^k_j > U^{\alpha}_s\right\}\right| \leq \left|\{i|\overline{z}^k_{si} > U^{\alpha}_s\}\right| < \alpha\,|\mathcal{I}_s|$, and this indicates that the upper DVC for $\alpha \in \overline{A}_s$ holds for any $\Xi_s \in \mathcal{Z}_s$. In regard to the lower DVCs, we can show it similarly.

Finally, we discuss Property (iii). From Property (i), there exists an optimal solution for any $k \geq 1$, thus it is sufficient to find a feasible solution in the $(k+1)$th LP whose objective value is t_k. We show that a feasible point in the $(k+1)$th LP can be constructed with $t = t_k,\ x_j = x^k_j,\ \overline{z}_{si} = \overline{z}^k_{si} = \sum_{j\in\mathcal{J}}[D_s + \delta|D^{'}_s|]_{ij}x^k_j,\ \underline{z}_{si} = \underline{z}^k_{si} = \sum_{j\in\mathcal{J}}[D_s - \delta|D'|]_{ij}x^k_j,\ \overline{\zeta}^{\alpha}_s = U^{\alpha}_s + \overline{P}^{\alpha}_s t_k,\ \underline{\zeta}^{\alpha}_s = L^{\alpha}_s - \underline{P}^{\alpha}_s t_k$. The objective value at this solution is $t = t_k$, and it is obvious that (8b), (8c), (8d) and (8e) hold in the $(k+1)$th LP, since these constraints are not affected by the updates of the hot and cold spots.

The constraint (8f) involves $\underline{R}^{\alpha}_{(k+1),s}$, but we can still show that

$$\begin{aligned}
&\underline{\zeta}^{\alpha}_s - \frac{1}{(1-\alpha)|\mathcal{I}_s| - |\underline{R}^{\alpha}_{(k+1),s}|}\sum_{i\in\mathcal{I}_s\setminus\underline{R}^{\alpha}_{(k+1),s}}(\underline{\zeta}^{\alpha}_s - \underline{z}_{si})^+ \\
&= L^{\alpha}_s - \underline{P}^{\alpha}_s t_k - \frac{1}{(1-\alpha)|\mathcal{I}_s| - |\underline{R}^{\alpha}_{(k+1),s}|}\sum_{i\in\mathcal{I}_s\setminus\underline{R}^{\alpha}_{(k+1),s}}(L^{\alpha}_s - \underline{P}^{\alpha}_s t_k - \underline{z}^k_{si})^+ \;=\; L^{\alpha}_s - \underline{P}^{\alpha}_s t_k.
\end{aligned}$$

Here, we used $(L^{\alpha}_s - \underline{P}^{\alpha}_s t_k - \underline{z}^k_{si})^+ = 0$ for each $i \in \mathcal{I}_s\setminus\underline{R}^{\alpha}_{(k+1),s}$, which is derived from $\underline{R}^{\alpha}_{(k+1),s} = \{i|\underline{z}^k_{si} < L^{\alpha}_s - \underline{P}^{\alpha}_s t_k\}$. In the same way, the inequality (8g) holds.

Therefore, we can find a feasible solution whose objective value is t_k. This indicates $t_{k+1} \leq t_k$ and completes the proof. □

3.3 The Proposed Method with Penalty Terms

Though SLPM can evaluate the deviation from DVCs by the optimal value t_k as discussed in [12], there remains voxels that receive much higher or lower doses. To reduce such voxel-wise deviations, we modify the objective function t in (8a) by adding penalty terms with thresholds $\underline{\theta}^{\alpha}_s, \overline{\theta}^{\alpha}_s, \underline{\theta}_s, \overline{\theta}_s > 0$ and weight parameters $\underline{\lambda}^{\alpha}_s, \overline{\lambda}^{\alpha}_s, \underline{\lambda}_s, \overline{\lambda}_s \geq 0$ as follows:

$$\begin{aligned}
t + &\sum_{s\in\mathcal{S},\alpha\in\underline{A}_s,i\in\mathcal{I}_s\setminus\underline{R}^{\alpha}_{k,s}}\frac{\underline{\lambda}^{\alpha}_s}{|\mathcal{I}_s| - |\underline{R}^{\alpha}_{k,s}|}(\underline{\theta}^{\alpha}_s - \underline{z}_{si})^+ + \sum_{s\in\mathcal{S},\alpha\in\overline{A}_s,i\in\mathcal{I}_s\setminus\overline{R}^{\alpha}_{k,s}}\frac{\overline{\lambda}^{\alpha}_s}{|\mathcal{I}_s| - |\overline{R}^{\alpha}_{k,s}|}(\overline{z}_{si} - \overline{\theta}^{\alpha}_s)^+ \\
&+ \sum_{s\in\mathcal{S},i\in\mathcal{I}_s}\frac{\underline{\lambda}_s}{|\mathcal{I}_s|}(\underline{\theta}_s - \underline{z}_{si})^+ + \sum_{s\in\mathcal{S},i\in\mathcal{I}_s}\frac{\overline{\lambda}_s}{|\mathcal{I}_s|}(\overline{z}_{si} - \overline{\theta}_s)^+. \qquad (10)
\end{aligned}$$

In addition, oncologists sometimes give a high priority on PTVs compared to healthy organs, and if there are plural PTVs, they prioritize a PTV that requires the highest absorbed dose.

As will be indicated in the numerical results in Section 4, the penalty terms improve the solution quality for some cases by reaching a region where the simple objective function t cannot search.

Table 1: Detailed information on TG119 datasets

	structures	PTV	$\lvert\mathcal{I}_s\rvert$	DVCs			DVC index	$\lvert\mathcal{J}\rvert$
C-Shape	Outer Target	✓	17522	$L^{0.95}_{\text{Outer Target}}$	=	50	1	414
				$U^{0.1}_{\text{Outer Target}}$	=	55	2	
	Core		3087	$U^{0.1}_{\text{Core}}$	=	25	3	
Head and Neck	PTV	✓	53994	$L^{0.99}_{\text{PTV}}$	=	46.5	1	619
				$L^{0.9}_{\text{PTV}}$	=	50	2	
				$U^{0.2}_{\text{PTV}}$	=	55	3	
	Cord		1333	U_{Cord}	=	40	4	
	Lt Parotid		525	$U^{0.5}_{\text{Lt Parotid}}$	=	20	5	
	Rt Parotid		740	$U^{0.5}_{\text{Rt Parotid}}$	=	20	6	
Prostate	Prostate PTV	✓	8591	$L^{0.95}_{\text{Prostate PTV}}$	=	75.6	1	241
				$U^{0.05}_{\text{Prostate PTV}}$	=	83	2	
	Bladder		5207	$U^{0.3}_{\text{Bladder}}$	=	70	3	
				$U^{0.1}_{\text{Bladder}}$	=	75	4	
	Rectum		1830	$U^{0.3}_{\text{Rectum}}$	=	70	5	
				$U^{0.1}_{\text{Rectum}}$	=	75	6	
MultiTarget	Center	✓	5143	$L^{0.99}_{\text{Center}}$	=	50	1	601
				$U^{0.1}_{\text{Center}}$	=	53	2	
	Superior	✓	5549	$L^{0.99}_{\text{Superior}}$	=	25	3	
				$U^{0.1}_{\text{Superior}}$	=	35	4	
	Inferior	✓	5529	$L^{0.99}_{\text{Inferior}}$	=	12.5	5	
				$U^{0.1}_{\text{Inferior}}$	=	25	6	

4 Numerical Experiments

In this section, we discuss numerical experiments of the proposed method (SLPM-R) compared to the existing method (SLPM). Our tests were performed on a Linux server with Opteron 4386 (3.10 GHz) and 128 GB memory space. We used CPLEX 12.6.2 to solve the LP problems (2) and (8). We performed the experiments under the same conditions as [12], so the number of LP problems solved successively is fixed at five ($K = 5$). We also used the same irradiation setting (the irradiations from five directions at 72 degrees each, $0°, 72°, 144°, 216°$ and $288°$), then we calculated the influence matrix D^0_s by the QIB method [11] with the default setting of CERR 3.0 [7].

We used test datasets named TG119 (Task Group 119) provided by AAPM (American Association of Physicists in Medicine) [10], which contains four datasets, C-Shape, Head and Neck, Prostate and MultiTarget. In Table 1, from the left to the right, the columns represent structure names, whether structures are PTVs (planning target volumes) or not, the number of voxels in each structure, the information of DVCs, the index numbers of DVCs that will be used in figures below, and the number of beamlets.

As mentioned in Section 3, the proposed method is focused on uncertainty in influence matrix of the form $D_s = D^0_s + \Xi_s \circ D'_s$ with $\Xi_s \in \mathcal{Z}_s$. We set the matrix D^0_s as the influence matrix computed with CERR. The range of $\mathcal{Z}_s$ is determined by the parameter δ which we change from 0.1 to 0.5. For preparing D'_s, let $\mathcal{P}_s = \{(i,j) | i = 1, \ldots, |\mathcal{I}_s|,\ j = 1, \ldots, |\mathcal{J}|\}$ be the index set of $D^0_s \in \mathbb{R}^{|\mathcal{I}_s| \times |\mathcal{J}|}$. We choose an index subset $\mathcal{P}'_s \subset \mathcal{P}_s$ randomly such that $|\mathcal{P}'_s| = \gamma |\mathcal{P}_s|$, where γ is a parameter $0 < \gamma \leq 1$. For each $(i,j) \in \mathcal{P}_s$, we take ε_{ij} from the normal distribution $\mathcal{N}(0,1)$, and we set $[D'_s]_{ij} = \min\{\max\{\varepsilon_{ij}, -1/\delta\}, 1/\delta\} D^0_s$. On the other hand, for $(i,j) \notin \mathcal{P}_s$, we simply set $[D'_s]_{ij} = 0$. Thus, each element of $D_s = D^0_s + \Xi_s \circ D'_s$ is nonnegative for any $\Xi_s \in \mathcal{Z}_s$. In the numerical experiments, we vary γ from 0.1 to 1. We set the parameters $\underline{P}^\alpha_s, \overline{P}^\alpha_s, \underline{P}_s, \overline{P}_s$ in the LP problems (2) and (8) as 1 in the same way as [12].

Table 2: Deviations from DVCs in C-Shape

			δ														
			0.1			0.2			0.3			0.4			0.5		
		DVCs	SLPM-R	minus	plus	SLPM-R	minus	plus	SLPM-R	minus	plus	SLPM-R	minus	plus	SLPM-R	minus	plus
γ	0.1	$L^{0.95}_{\text{Outer Target}} = 50$	-0.31	-0.81	-0.00	0.08	-0.92	0.80	0.35	-1.17	1.63	0.59	-1.42	2.35	0.89	-1.60	3.11
		$U^{0.1}_{\text{Outer Target}} = 55$	-0.39	0.04	-0.89	-0.14	0.85	-1.24	0.16	1.67	-1.58	0.56	2.63	-1.87	0.85	3.56	-2.11
		$U^{0.1}_{\text{Core}} = 25$	-0.05	-0.25	-0.61	0.69	0.41	-0.49	1.45	1.15	-0.29	2.48	1.92	0.11	3.19	2.81	0.13
	0.2	$L^{0.95}_{\text{Outer Target}} = 50$	-0.15	-1.09	0.60	0.19	-1.67	1.83	0.67	-2.17	3.16	0.91	-2.73	4.34	1.35	-3.44	5.44
		$U^{0.1}_{\text{Outer Target}} = 55$	-0.34	0.60	-1.30	0.11	2.07	-1.83	0.50	3.63	-2.61	0.86	5.19	-3.10	1.47	7.27	-3.62
		$U^{0.1}_{\text{Core}} = 25$	0.32	0.10	-0.62	1.38	1.28	-0.48	2.96	2.80	-0.06	3.92	4.18	0.02	5.05	5.62	0.19
	0.3	$L^{0.95}_{\text{Outer Target}} = 50$	-0.11	-1.42	1.01	0.49	-2.22	2.82	0.79	-3.24	4.40	1.31	-4.34	6.00	1.78	-5.17	7.46
		$U^{0.1}_{\text{Outer Target}} = 55$	-0.30	1.08	-1.63	0.19	3.19	-2.54	0.67	5.41	-3.44	1.26	7.96	-4.21	1.85	10.41	-4.86
		$U^{0.1}_{\text{Core}} = 25$	0.60	0.44	-0.80	2.11	2.14	-0.56	3.64	3.93	-0.50	5.27	6.06	-0.24	6.69	8.06	-0.21
	0.4	$L^{0.95}_{\text{Outer Target}} = 50$	-0.12	-1.79	1.45	0.57	-2.98	3.59	1.04	-4.42	5.61	1.65	-5.63	7.60	2.32	-7.27	9.36
		$U^{0.1}_{\text{Outer Target}} = 55$	-0.28	1.62	-1.96	0.28	4.29	-3.20	0.81	7.29	-4.26	1.56	10.64	-5.28	2.28	14.15	-6.12
		$U^{0.1}_{\text{Core}} = 25$	0.83	0.63	-0.90	2.57	2.79	-0.87	4.21	5.05	-0.78	6.05	7.77	-0.72	7.45	10.71	-0.93
	0.5	$L^{0.95}_{\text{Outer Target}} = 50$	-0.00	-2.11	2.00	0.52	-3.91	4.41	1.34	-5.50	6.80	1.98	-7.52	8.89	2.80	-9.55	11.07
		$U^{0.1}_{\text{Outer Target}} = 55$	-0.24	2.21	-2.33	0.44	5.65	-3.80	1.06	9.36	-5.09	1.79	13.53	-6.18	2.71	18.20	-7.24
		$U^{0.1}_{\text{Core}} = 25$	1.04	0.91	-1.08	3.15	3.58	-1.09	5.16	6.61	-1.12	6.74	9.76	-1.08	8.42	13.68	-1.62
	0.6	$L^{0.95}_{\text{Outer Target}} = 50$	0.06	-2.50	2.33	0.64	-4.76	5.10	1.46	-6.84	7.85	2.21	-9.49	10.26	3.17	-12.07	12.70
		$U^{0.1}_{\text{Outer Target}} = 55$	-0.26	2.64	-2.71	0.40	6.83	-4.40	1.20	11.31	-5.90	2.03	16.66	-7.26	2.91	22.59	-8.49
		$U^{0.1}_{\text{Core}} = 25$	1.29	1.29	-1.00	3.74	4.43	-1.12	5.61	7.48	-1.65	7.58	11.34	-1.76	9.30	15.79	-1.93
	0.7	$L^{0.95}_{\text{Outer Target}} = 50$	0.07	-2.93	2.74	0.87	-5.34	5.95	1.65	-8.23	8.83	2.50	-11.53	11.53	3.39	-15.11	13.98
		$U^{0.1}_{\text{Outer Target}} = 55$	-0.19	3.28	-3.02	0.47	7.92	-4.99	1.30	13.35	-6.74	2.19	19.80	-8.26	3.11	27.34	-9.55
		$U^{0.1}_{\text{Core}} = 25$	1.47	1.52	-1.31	3.70	4.65	-1.78	5.93	8.83	-2.13	7.93	13.24	-2.72	10.35	19.43	-2.77
	0.8	$L^{0.95}_{\text{Outer Target}} = 50$	0.10	-3.32	3.12	1.02	-6.24	6.67	1.84	-9.75	9.90	2.94	-13.69	12.72	4.10	-18.19	15.42
		$U^{0.1}_{\text{Outer Target}} = 55$	-0.21	3.80	-3.36	0.58	9.27	-5.60	1.51	15.70	-7.55	2.39	23.49	-9.17	3.41	32.27	-10.71
		$U^{0.1}_{\text{Core}} = 25$	1.64	1.71	-1.64	4.19	5.40	-2.10	6.48	10.06	-2.55	8.76	15.66	-3.09	10.59	22.45	-3.59
	0.9	$L^{0.95}_{\text{Outer Target}} = 50$	0.17	-3.76	3.52	1.12	-7.27	7.35	2.12	-11.20	10.86	3.00	-16.28	13.88	4.27	-22.07	16.67
		$U^{0.1}_{\text{Outer Target}} = 55$	-0.22	4.35	-3.69	0.60	10.55	-6.22	1.60	18.18	-8.30	2.70	27.43	-10.08	3.63	38.78	-11.80
		$U^{0.1}_{\text{Core}} = 25$	1.87	2.01	-1.72	4.43	6.13	-2.52	6.88	11.37	-2.96	9.17	18.46	-3.55	11.21	26.79	-4.30
	1.0	$L^{0.95}_{\text{Outer Target}} = 50$	0.17	-4.17	3.93	1.14	-8.23	8.04	2.21	-12.96	11.79	3.30	-19.11	14.91	4.53	-26.61	17.89
		$U^{0.1}_{\text{Outer Target}} = 55$	-0.14	4.92	-4.03	0.72	11.95	-6.75	1.71	20.57	-9.06	2.74	31.60	-11.05	3.85	45.69	-12.72
		$U^{0.1}_{\text{Core}} = 25$	2.20	2.33	-1.79	4.65	6.78	-2.90	7.32	12.23	-3.49	9.79	20.52	-3.98	11.55	30.12	-5.15

4.1 Numerical Results

We first report numerical results of SLPM-R with the simple objective function t of (8a).

C-Shape

Table 2 shows the deviations from the DVCs. The column of "SLPM-R" represents the deviation of the proposed method while the columns of "minus" and "plus" represent the deviations of the existing method (SLPM) with the worst cases of uncertainty. More precisely, these two deviations correspond to the results of SLPM with the influence matrices $D^0_s - \delta|D'_s|$ and $D^0_s + \delta|D'_s|$. These two cases of SLPM, hereafter, are referred as the worst cases. In Table 2, a DVC is satisfied if the corresponding value is nonpositive. For example, the value -0.31 at the column of SLPM-R at $(\gamma, \delta) = (0.1, 0.1)$ with respect to $L^{0.95}_{\text{Outer Target}} = 50$ indicates that more than 95 % of the voxels in Outer Target receive 50.31 Gy or more, thus the DVC $L^{0.95}_{\text{Outer Target}} = 50$ is satisfied. We use nonpositive values to indicate the satisfaction of DVCs, since Property (ii) in Proposition 2 indicates that when $t_k \leq 0$, the obtained solution x^k satisfies all DVCs.

For the smallest pair of parameters $(\gamma, \delta) = (0.1, 0.1)$, SLPM-R can find a solution that satisfies all DVCs, but the minimum case of SLPM cannot. For larger parameters, the results do not always satisfy all DVCs, since it is more difficult to satisfy all DVCs when the data includes more uncertainty.

The left and right figures in Figure 2 illustrate DVHs for parameter pairs $(\gamma, \delta) = (0.5, 0.2)$ and $(\gamma, \delta) = (0.5, 0.5)$, respectively. In the left figure, the left and right solid curves are the DVHs by SLPM-R for Outer Target and Core, respectively. Each area surrounded by two thin curves is the area obtained by SLPM with the worst cases, $D^0_s - \delta|D'_s|$ and $D^0_s + \delta|D'_s|$.

In the left figure, both SLPM and SLPM-R cannot fulfill all the three DVCs, but SLPM-R obtains a favorable solution. Let us here focus a DVC of $U^{0.1}_{\text{Outer Target}} = 55$. The range of the worst

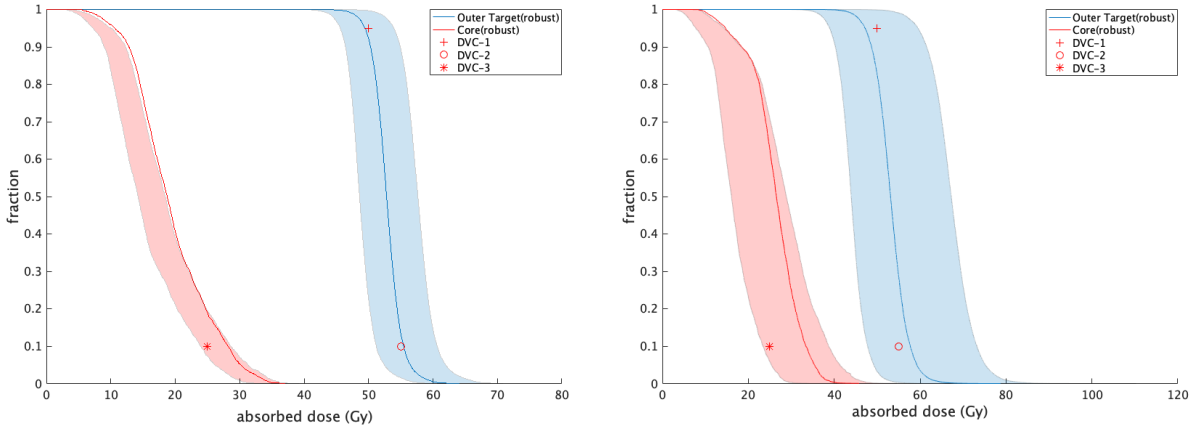

Figure 2: DVHs on C-Shape with $(\gamma, \delta) = (0.5, 0.2)$ (left) and $(\gamma, \delta) = (0.5, 0.5)$ (right), respectively

cases at fraction $\alpha = 0.1$ is from 51.20 Gy to 60.65 Gy, and it includes the DVC point 55 Gy. In contrast, the DVH of SLPM-R (the solid curve) passes the point 55.44 Gy at fraction $\alpha = 0.1$, which is close to 55 Gy when we consider the above range from 51.20 Gy to 60.65 Gy. There is often a trade-off among the deviations of multiple DVCs, therefore, if we can make a difference from one DVC small, it is often easier to make the deviations from other DVCs smaller. In other words, if we satisfy one DVC too much (except cases where we give a high priority on a specific DVC in Section 4.2 later), it makes it difficult to satisfy the other DVCs. Actually, the largest deviations in SLPM are 5.65 Gy and 4.41 Gy for $D_s^0 - \delta|D_s'|$ and $D_s^0 + \delta|D_s'|$, respectively, but it is 3.15 Gy in SLPM-R. Though we give only D_s^0 and δ to both SLPM and SLPM-R, Figure 2 indicates that SLPM-R can find a better solution than SLPM.

The right figure of Figure 2 is a result with respect to $(\gamma, \delta) = (0.5, 0.5)$. Due to the larger uncertainty, the ranges sandwiched the worst cases in the existing method turn out to be wider. In SLPM-R, the deviation from the DVC $U^{0.1}_{\text{Outer Target}} = 55$ becomes worse slightly, but the solid curve still passes near the DVC point and the largest deviation in the three DVCs is small compared to SLPM.

Head and Neck

In the Head and Neck dataset, PTV has 53994 voxels, and this dataset is the largest in TG119. If we construct successive five LP problems with all voxels, a heavy computation cost is necessary. We randomly picked up 10000 voxels from PTV and OARs, since it was reported in [12] that this size reduction does not remarkably affect the computed DVHs for the Head and Neck dataset.

Table 3 reports the deviations from DVCs. Both SLPM and SLPM-R find a solution that satisfies all DVCs when γ and δ are small. In contrast, when $(\gamma, \delta) = (0.6, 0.1)$ and $(\gamma, \delta) = (0.2, 0.2)$, SLPM-R outputs a solution satisfying all DVCs, but SLPM does not.

In Figure 3, we show two DVHs of parameter pairs $(\gamma, \delta) = (0.2, 0.2)$ and $(\gamma, \delta) = (0.8, 0.2)$. When $(\gamma, \delta) = (0.2, 0.2)$, we can see the solution of SLPM-R satisfies all DVCs, since the parameters regarding uncertainty are relatively small. On the other hand, when $(\gamma, \delta) = (0.8, 0.2)$, it is hard for even SLPM-R to find a feasible solution that satisfies all DVCs, since most components of influence matrix contain the errors. Especially, DVCs of Lt Parotid and Rt Parotid are severer than those of PTV and Cord. In the next subsection, we will show that the proposed method with the penalty terms of Section 3.3 can find a solution.

Table 3: Deviations from DVCs in Head and Neck

				δ														
				0.1			0.2			0.3			0.4			0.5		
		DVCs		SLPM-R	minus	plus	SLPM-R	minus	plus	SLPM-R	minus	plus	SLPM-R	minus	plus	SLPM-R	minus	plus
γ	0.1	$L^{0.9}_{\text{PTV}}$	= 50	-1.23	-1.65	-0.89	-0.98	-1.86	-0.34	-0.62	-2.02	0.28	-0.31	-2.27	0.88	0.07	-2.50	1.43
		$L^{0.99}_{\text{PTV}}$	= 46.5	-1.69	-2.21	-1.33	-1.68	-2.47	-0.73	-1.01	-2.13	0.34	-0.68	-2.63	1.12	0.46	-1.91	2.03
		$U^{0.2}_{\text{PTV}}$	= 55	-1.26	-0.87	-1.73	-1.06	-0.25	-2.01	-0.63	0.57	-2.19	-0.18	1.38	-2.39	0.55	2.69	-2.70
		U_{Cord}	= 40	-0.77	-0.50	-1.23	-0.12	0.64	-1.13	-0.26	2.47	-0.94	-0.41	7.36	-0.85	-0.65	9.76	-1.43
		$U^{0.5}_{\text{Lt\_Parotid}}$	= 20	-1.95	-2.10	-2.53	-1.55	-1.50	-2.17	-0.09	-0.55	-1.78	0.24	0.38	-1.85	1.88	1.27	-1.82
		$U^{0.5}_{\text{Rt\_Parotid}}$	= 20	-1.71	-1.91	-1.84	-1.33	-1.75	-2.38	-0.14	-1.09	-2.22	0.59	-0.10	-1.66	1.25	0.87	-1.92
	0.2	$L^{0.9}_{\text{PTV}}$	= 50	-1.20	-2.03	-0.45	-0.74	-2.53	0.70	-0.32	-3.07	1.75	0.15	-3.56	2.77	0.89	-3.85	3.77
		$L^{0.99}_{\text{PTV}}$	= 46.5	-1.70	-2.61	-0.73	-1.20	-3.01	0.57	-0.54	-2.96	2.09	0.49	-2.80	3.43	1.57	-2.60	4.33
		$U^{0.2}_{\text{PTV}}$	= 55	-1.23	-0.43	-2.08	-0.79	0.98	-2.65	-0.25	2.44	-3.17	0.63	4.36	-3.65	1.42	6.55	-4.08
		U_{Cord}	= 40	-0.54	1.04	-1.40	-0.54	1.88	-1.23	-0.69	3.12	-1.04	-1.58	4.64	-0.77	-0.35	8.12	-2.29
		$U^{0.5}_{\text{Lt\_Parotid}}$	= 20	-1.42	-1.38	-2.26	-0.23	-0.46	-2.22	1.28	0.44	-1.79	2.37	2.51	-2.04	4.22	4.12	-1.55
		$U^{0.5}_{\text{Rt\_Parotid}}$	= 20	-1.77	-1.88	-2.38	-0.77	-0.87	-2.45	0.96	0.51	-2.13	1.96	2.06	-1.81	3.97	3.89	-1.46
	0.3	$L^{0.9}_{\text{PTV}}$	= 50	-1.04	-2.37	0.12	-0.56	-3.34	1.62	-0.00	-4.13	3.14	0.50	-5.15	4.47	1.09	-5.88	5.88
		$L^{0.99}_{\text{PTV}}$	= 46.5	-1.74	-2.76	-0.50	-1.20	-3.87	1.45	-0.25	-4.06	3.15	1.13	-3.82	5.09	2.84	-3.68	6.99
		$U^{0.2}_{\text{PTV}}$	= 55	-1.12	0.19	-2.42	-0.65	2.11	-3.37	0.04	4.28	-4.05	0.88	7.13	-4.81	1.87	9.92	-5.44
		U_{Cord}	= 40	-0.40	0.41	-1.37	-0.80	7.08	-1.56	-0.71	5.52	-1.07	-2.52	7.91	-2.33	-1.23	13.53	-2.84
		$U^{0.5}_{\text{Lt\_Parotid}}$	= 20	-1.00	-1.84	-2.61	0.34	0.04	-2.30	2.25	1.82	-2.17	4.19	4.32	-1.87	5.61	6.46	-1.29
		$U^{0.5}_{\text{Rt\_Parotid}}$	= 20	-1.48	-1.79	-2.45	0.58	-0.12	-2.19	2.37	1.18	-2.01	3.55	3.73	-1.78	5.20	6.84	-1.74
	0.4	$L^{0.9}_{\text{PTV}}$	= 50	-1.04	-2.78	0.42	-0.40	-4.01	2.45	0.19	-5.40	4.32	0.73	-6.76	6.09	1.74	-7.80	7.70
		$L^{0.99}_{\text{PTV}}$	= 46.5	-1.97	-3.27	-0.03	-1.05	-4.43	2.01	0.40	-4.69	4.61	1.51	-5.34	6.50	3.56	-5.17	8.80
		$U^{0.2}_{\text{PTV}}$	= 55	-1.14	0.60	-2.87	-0.51	3.24	-3.93	0.17	6.29	-5.01	1.09	9.76	-5.92	2.10	13.86	-6.81
		U_{Cord}	= 40	-0.83	1.03	-1.75	-1.73	3.58	-1.93	-2.62	7.51	-2.39	-2.63	8.40	-3.29	-3.35	17.16	-4.83
		$U^{0.5}_{\text{Lt\_Parotid}}$	= 20	-0.53	-1.47	-2.34	1.05	0.88	-2.26	3.22	2.54	-2.23	5.13	5.42	-1.99	6.76	8.39	-2.42
		$U^{0.5}_{\text{Rt\_Parotid}}$	= 20	-0.85	-1.50	-2.71	0.81	0.41	-2.75	2.95	2.69	-2.37	4.55	5.38	-2.23	7.00	7.66	-1.94
	0.5	$L^{0.9}_{\text{PTV}}$	= 50	-0.89	-3.09	0.91	-0.34	-4.88	3.27	0.28	-6.67	5.43	0.98	-8.61	7.47	1.77	-10.89	9.37
		$L^{0.99}_{\text{PTV}}$	= 46.5	-1.74	-3.32	0.68	-0.87	-5.23	2.85	0.38	-6.18	5.29	1.88	-6.94	7.94	3.71	-6.96	10.40
		$U^{0.2}_{\text{PTV}}$	= 55	-1.06	1.20	-3.17	-0.44	4.33	-4.64	0.37	8.14	-5.86	1.27	12.74	-7.03	2.39	18.09	-8.08
		U_{Cord}	= 40	-1.03	2.45	-1.88	-2.14	5.29	-2.42	-2.15	8.87	-2.46	-4.21	9.02	-3.67	-2.87	14.82	-1.59
		$U^{0.5}_{\text{Lt\_Parotid}}$	= 20	-0.55	-1.14	-2.81	1.72	0.51	-2.50	4.14	3.71	-2.56	6.32	6.46	-2.63	8.11	11.28	-2.77
		$U^{0.5}_{\text{Rt\_Parotid}}$	= 20	-0.52	-1.20	-2.99	1.45	0.85	-2.54	3.51	3.74	-2.62	5.68	6.63	-2.60	8.04	10.88	-2.54
	0.6	$L^{0.9}_{\text{PTV}}$	= 50	-0.87	-3.52	1.34	-0.04	-5.62	4.06	0.64	-7.93	6.63	1.52	-10.29	8.89	2.48	-13.58	11.04
		$L^{0.99}_{\text{PTV}}$	= 46.5	-1.36	-3.94	1.01	-0.18	-5.60	3.95	1.03	-7.04	6.96	2.70	-8.22	9.72	4.62	-9.14	12.07
		$U^{0.2}_{\text{PTV}}$	= 55	-1.05	1.70	-3.51	-0.39	5.60	-5.21	0.58	10.48	-6.70	1.53	16.06	-8.06	2.61	23.06	-9.43
		U_{Cord}	= 40	-0.83	2.12	-1.70	-2.16	5.08	-2.70	-3.79	15.22	-2.91	-3.83	17.64	-3.41	-4.72	28.35	-4.82
		$U^{0.5}_{\text{Lt\_Parotid}}$	= 20	-0.52	-1.01	-3.06	2.03	2.01	-2.87	4.53	4.85	-2.75	6.62	9.18	-2.79	9.31	14.09	-2.54
		$U^{0.5}_{\text{Rt\_Parotid}}$	= 20	-0.31	-0.98	-2.86	1.68	1.73	-2.97	4.85	4.29	-2.90	6.91	8.75	-2.64	9.23	14.46	-3.38
	0.7	$L^{0.9}_{\text{PTV}}$	= 50	-0.80	-3.92	1.77	0.03	-6.47	4.82	0.92	-9.44	7.54	1.74	-12.49	10.12	3.09	-16.22	12.53
		$L^{0.99}_{\text{PTV}}$	= 46.5	-1.55	-4.67	1.06	-0.30	-6.74	4.14	1.44	-8.56	7.34	3.52	-9.07	11.00	5.16	-11.77	13.71
		$U^{0.2}_{\text{PTV}}$	= 55	-1.01	2.22	-3.93	-0.29	6.75	-5.82	0.61	12.25	-7.68	1.58	19.58	-9.26	2.83	28.20	-10.57
		U_{Cord}	= 40	-1.44	2.34	-2.38	-2.23	7.02	-2.46	-4.69	11.30	-3.68	-4.74	15.10	-4.01	-5.94	21.78	-6.32
		$U^{0.5}_{\text{Lt\_Parotid}}$	= 20	-0.07	-0.45	-2.92	2.67	1.86	-3.05	4.90	5.60	-2.95	8.28	10.63	-3.25	10.58	16.63	-3.71
		$U^{0.5}_{\text{Rt\_Parotid}}$	= 20	0.04	-1.06	-2.98	2.44	1.84	-2.97	4.93	5.81	-3.32	7.73	10.44	-3.38	9.56	17.16	-4.14
	0.8	$L^{0.9}_{\text{PTV}}$	= 50	-0.75	-4.32	2.20	0.13	-7.55	5.55	0.85	-11.04	8.50	1.84	-15.25	11.27	3.18	-19.96	13.85
		$L^{0.99}_{\text{PTV}}$	= 46.5	-1.08	-4.92	1.59	-0.37	-7.78	4.99	1.43	-9.56	8.94	3.51	-11.53	11.70	5.78	-13.96	14.66
		$U^{0.2}_{\text{PTV}}$	= 55	-0.98	2.77	-4.23	-0.22	7.90	-6.50	0.56	14.44	-8.56	1.61	23.02	-10.33	2.98	33.95	-11.73
		U_{Cord}	= 40	-1.86	3.43	-2.78	-3.51	9.35	-2.99	-4.95	15.28	-4.28	-5.72	18.88	-5.43	-6.55	23.66	-6.73
		$U^{0.5}_{\text{Lt\_Parotid}}$	= 20	0.27	-0.68	-3.01	3.22	2.75	-3.05	5.31	6.35	-3.73	8.03	10.70	-3.72	11.07	20.26	-3.94
		$U^{0.5}_{\text{Rt\_Parotid}}$	= 20	0.26	-0.16	-3.30	3.26	2.48	-3.16	5.06	6.19	-3.50	7.89	11.70	-4.06	10.66	20.05	-4.48
	0.9	$L^{0.9}_{\text{PTV}}$	= 50	-0.70	-4.77	2.54	0.28	-8.33	6.29	1.09	-12.57	9.46	2.03	-17.69	12.42	3.53	-24.15	15.23
		$L^{0.99}_{\text{PTV}}$	= 46.5	-1.32	-5.14	1.92	0.28	-8.00	5.72	1.66	-11.22	9.53	3.74	-14.38	12.62	6.18	-16.97	16.01
		$U^{0.2}_{\text{PTV}}$	= 55	-0.90	3.28	-4.54	-0.16	9.25	-7.08	0.62	16.69	-9.34	1.56	26.25	-11.31	2.77	39.59	-12.93
		U_{Cord}	= 40	-2.22	3.08	-2.80	-3.28	9.20	-3.92	-3.49	13.24	-5.46	-5.77	22.41	-5.88	-3.74	26.90	-7.02
		$U^{0.5}_{\text{Lt\_Parotid}}$	= 20	0.57	-0.49	-3.00	3.17	2.82	-3.53	6.25	8.25	-3.83	8.48	12.22	-4.43	11.38	22.87	-4.60
		$U^{0.5}_{\text{Rt\_Parotid}}$	= 20	0.43	-0.08	-2.85	3.49	3.09	-3.48	5.87	7.05	-4.01	8.59	12.87	-4.64	11.05	22.80	-4.97
	1.0	$L^{0.9}_{\text{PTV}}$	= 50	-0.68	-5.21	2.93	0.42	-9.30	6.97	1.30	-14.48	10.40	2.43	-20.53	13.56	4.35	-28.40	16.42
		$L^{0.99}_{\text{PTV}}$	= 46.5	-1.09	-5.41	2.20	0.15	-9.19	6.46	2.17	-12.80	10.29	4.27	-15.88	14.12	7.09	-20.81	17.13
		$U^{0.2}_{\text{PTV}}$	= 55	-0.95	3.77	-4.95	-0.12	10.51	-7.71	0.71	19.06	-10.14	1.81	31.25	-12.22	2.78	47.14	-14.03
		U_{Cord}	= 40	-2.23	4.44	-2.72	-3.69	9.99	-3.77	-5.02	15.85	-3.49	-6.22	22.19	-6.64	-8.03	29.41	-6.20
		$U^{0.5}_{\text{Lt\_Parotid}}$	= 20	0.76	0.02	-2.88	3.85	3.77	-4.12	6.95	8.49	-3.80	9.71	16.49	-4.75	12.10	25.57	-5.19
		$U^{0.5}_{\text{Rt\_Parotid}}$	= 20	0.79	0.01	-3.60	3.61	3.00	-3.77	6.97	8.23	-4.32	9.08	15.92	-4.74	11.23	27.01	-5.17

Prostate

Table 4 shows the deviations from DVCs regarding the dataset of Prostate. When the parameters γ and δ are small, SLPM-R again outputs the solution satisfying all DVCs. From the table, we can observe that the lower DVC of Prostate and the DVCs of Rectum are in a relation of trade-off, therefore, it is difficult to find a solution satisfying all DVCs. In contrast, DVCs of Bladder are easily satisfied.

This dataset requires the highest doses among the four datasets while the number of beamlets

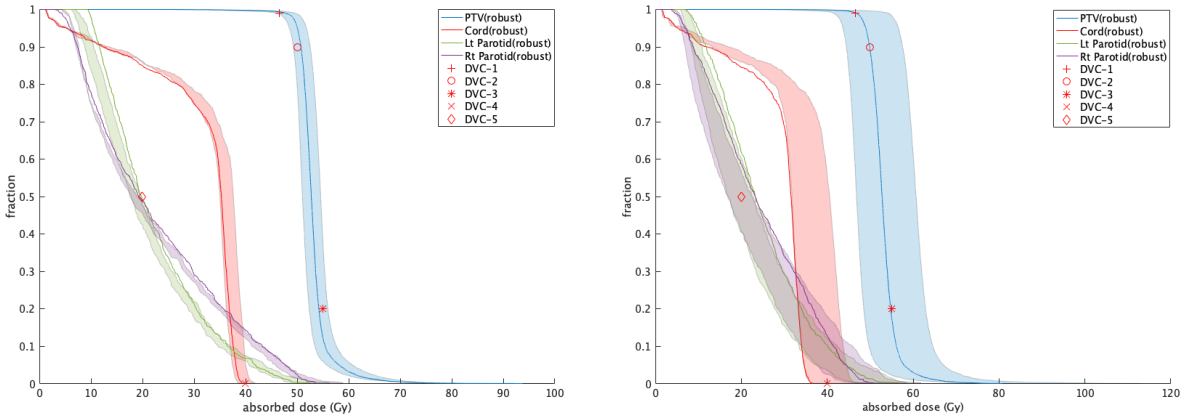

Figure 3: DVHs of Head and Neck with $(\gamma, \delta) = (0.2, 0.2)$ (left) and $(\gamma, \delta) = (0.8, 0.2)$ (right), respectively.

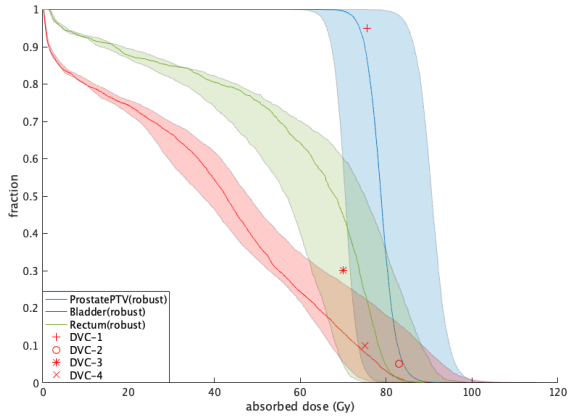

Figure 4: DVHs of Prostate with parameters $(\gamma, \delta) = (0.5, 0.3)$

is the least, therefore, uncertainty in the influence matrix affects the results largely. In fact, when $(\gamma, \delta) = (0.5, 0.3)$ in Figure 4, the deviations of SLPM-R for Prostate PTV are at most 3.75 Gy, while the largest deviations in the worst cases of SLPM are 13.29 Gy and 9.43 Gy, respectively.

MultiTarget

As shown in Table 1, all three structures in this dataset are PTVs, and each PTV sets lower and upper DVCs. In Table 5, we observe that both SLPM and SLPM-R cannot fulfill all six DVCs. The difficulty of this dataset was already discussed in [12]. When we focus the case of $(\gamma, \delta) = (0.5, 0.2)$, the largest deviations of the two worst cases by SLPM are 7.54 Gy and 6.37 Gy, but that by SLPM-R is 6.17 Gy. Therefore, SLPM-R can reduce the largest deviations of the worst cases.

We confirm in Table 5 that Superior and Inferior are strongly affected by uncertainty. Since the irradiation is performed on the coordinate plane of $z = 0$ and only Center exists on that plane, Superior and Inferior are subject to large error in uncertainty. Since we discuss FMO with given beam angles in this paper, this argument is beyond the range of this paper, but one of resolutions would be to conduct irradiations from the other angles such as the coordinate plane of $y = 0$.

Table 4: Derivations from DVCs in Prostate

			δ															
			0.1			0.2			0.3			0.4			0.5			
		DVCs	SLPM-R	minus	plus	SLPM-R	minus	plus	SLPM-R	minus	plus	SLPM-R	minus	plus	SLPM-R	minus	plus	
γ	0.1	$L^{0.95}_{\text{Prostate PTV}} = 75.6$	-0.82	-1.47	-0.27	-0.69	-1.89	0.80	-0.26	-2.29	1.84	0.05	-2.97	3.00	0.11	-3.52	3.97	
		$U^{0.05}_{\text{Prostate PTV}} = 83$	-1.00	-0.27	-1.83	-1.03	0.65	-2.50	-1.00	1.95	-3.47	-0.51	3.25	-4.03	-0.04	4.60	-4.78	
		$U^{0.30}_{\text{Bladder}} = 70$	-17.87	-17.06	-20.94	-18.15	-17.30	-26.60	-16.98	-13.33	-16.98	-13.97	-13.26	-16.45	-13.64	-12.80	-20.14	
		$U^{0.10}_{\text{Bladder}} = 75$	-1.95	-1.25	-2.63	-1.29	0.13	-2.49	-0.30	1.63	-2.40	0.83	2.61	-2.47	0.76	4.05	-2.86	
		$U^{0.30}_{\text{Rectum}} = 70$	-2.45	-1.13	-2.63	-0.55	-0.52	-2.99	0.40	1.67	-2.70	0.91	2.82	-3.25	2.63	4.04	-1.82	
		$U^{0.10}_{\text{Rectum}} = 75$	-0.76	-0.28	-1.39	-0.04	0.71	-1.62	0.78	1.98	-1.56	1.25	3.26	-2.17	2.73	4.53	-1.73	
	0.2	$L^{0.95}_{\text{Prostate PTV}} = 75.6$	-0.75	-2.06	0.43	-0.53	-3.16	2.16	-0.07	-4.16	3.94	0.64	-5.10	5.78	2.04	-6.00	7.69	
		$U^{0.05}_{\text{Prostate PTV}} = 83$	-1.11	0.32	-2.42	-0.96	2.29	-3.80	-0.45	4.60	-4.82	0.45	7.32	-5.66	1.66	9.83	-6.33	
		$U^{0.30}_{\text{Bladder}} = 70$	-14.86	-10.51	-20.83	-13.84	-10.42	-19.70	-10.92	-10.65	-17.20	-9.30	-7.69	-20.81	-11.06	-3.67	-13.85	
		$U^{0.10}_{\text{Bladder}} = 75$	-1.70	-0.78	-3.00	-0.47	1.89	-3.28	-0.21	3.59	-4.61	2.38	6.32	-3.87	0.10	8.96	-3.72	
		$U^{0.30}_{\text{Rectum}} = 70$	-1.37	-0.59	-2.77	0.15	1.57	-3.26	0.92	4.05	-3.57	3.02	6.18	-3.58	4.67	8.12	-3.88	
		$U^{0.10}_{\text{Rectum}} = 75$	-0.57	0.67	-1.83	0.32	2.41	-2.40	1.58	4.80	-2.61	2.98	7.21	-2.67	4.62	9.57	-3.14	
	0.3	$L^{0.95}_{\text{Prostate PTV}} = 75.6$	-0.79	-2.68	1.05	-0.32	-4.32	3.57	0.34	-5.80	5.83	1.85	-7.24	8.31	6.24	-9.23	10.70	
		$U^{0.05}_{\text{Prostate PTV}} = 83$	-1.10	1.15	-3.04	-0.81	3.89	-4.84	0.11	7.26	-6.07	1.09	11.20	-7.07	-0.90	15.18	-8.07	
		$U^{0.30}_{\text{Bladder}} = 70$	-18.76	-14.85	-18.96	-13.69	-14.81	-17.34	-11.52	-8.47	-19.30	-12.49	-3.33	-18.40	-10.69	0.34	-13.81	
		$U^{0.10}_{\text{Bladder}} = 75$	-1.76	0.21	-2.94	0.16	3.15	-4.39	1.36	6.58	-5.34	-0.48	11.59	-5.02	-1.54	12.86	-5.48	
		$U^{0.30}_{\text{Rectum}} = 70$	-2.01	-0.05	-3.67	0.48	3.34	-3.50	1.97	5.87	-4.23	3.91	9.89	-4.47	5.10	13.58	-5.36	
		$U^{0.10}_{\text{Rectum}} = 75$	-0.20	1.39	-2.14	0.74	4.10	-3.33	2.10	7.05	-4.02	4.07	10.97	-4.29	3.69	14.95	-5.67	
	0.4	$L^{0.95}_{\text{Prostate PTV}} = 75.6$	-0.73	-3.18	1.74	-0.02	-5.41	4.73	1.02	-7.54	7.75	4.57	-9.71	10.71	9.69	-11.63	13.62	
		$U^{0.05}_{\text{Prostate PTV}} = 83$	-1.10	1.91	-3.53	-0.56	5.73	-5.74	0.45	10.24	-7.17	0.04	15.37	-8.48	-3.14	20.47	-9.73	
		$U^{0.30}_{\text{Bladder}} = 70$	-17.10	-18.39	-19.79	-14.12	-10.07	-20.05	-5.45	-4.53	-18.03	-18.48	-1.18	-19.15	-12.12	5.91	-19.89	
		$U^{0.10}_{\text{Bladder}} = 75$	-0.97	0.96	-3.58	0.46	4.72	-4.72	1.65	10.76	-6.02	-4.77	14.61	-6.69	-5.27	20.02	-8.12	
		$U^{0.30}_{\text{Rectum}} = 70$	-1.63	0.81	-4.28	0.61	5.42	-4.38	2.68	9.09	-5.39	5.22	13.51	-6.70	2.13	19.17	-7.16	
		$U^{0.10}_{\text{Rectum}} = 75$	-0.31	1.89	-2.70	0.94	5.88	-4.27	2.59	9.83	-5.15	4.12	15.35	-5.96	1.40	20.57	-7.64	
	0.5	$L^{0.95}_{\text{Prostate PTV}} = 75.6$	-0.68	-3.82	2.32	0.06	-6.63	5.96	1.80	-9.51	9.43	7.37	-12.10	13.10	12.44	-15.09	16.11	
		$U^{0.05}_{\text{Prostate PTV}} = 83$	-1.06	2.57	-4.18	-0.41	7.34	-6.54	1.03	13.11	-8.46	-1.68	19.69	-10.00	-5.04	27.05	-11.24	
		$U^{0.30}_{\text{Bladder}} = 70$	-16.11	-10.95	-19.94	-12.44	-11.54	-16.32	-15.02	-4.70	-17.23	-14.82	3.01	-22.05	-18.49	9.29	-18.05	
		$U^{0.10}_{\text{Bladder}} = 75$	-1.52	2.08	-4.29	-0.21	6.94	-5.90	-1.84	13.29	-7.88	-3.70	19.50	-9.79	-11.03	24.40	-10.04	
		$U^{0.30}_{\text{Rectum}} = 70$	-0.71	1.23	-3.77	0.47	6.30	-6.08	3.75	11.53	-7.33	3.86	17.59	-7.37	-0.54	25.14	-9.83	
		$U^{0.10}_{\text{Rectum}} = 75$	-0.30	2.53	-3.43	1.15	7.42	-5.22	3.19	13.24	-6.67	2.74	19.73	-7.42	-1.71	26.78	-9.51	
	0.6	$L^{0.95}_{\text{Prostate PTV}} = 75.6$	-0.69	-4.54	2.97	0.30	-7.82	7.17	3.25	-11.46	11.12	9.70	-14.80	14.94	14.92	-18.58	18.38	
		$U^{0.05}_{\text{Prostate PTV}} = 83$	-0.93	3.45	-4.68	-0.10	9.24	-7.50	-0.03	16.45	-9.60	-3.66	24.31	-11.32	-7.23	33.05	-13.03	
		$U^{0.30}_{\text{Bladder}} = 70$	-15.49	-14.44	-21.20	-13.29	-7.34	-19.34	-13.76	2.47	-23.86	-20.16	4.39	-18.88	-16.82	13.50	-16.85	
		$U^{0.10}_{\text{Bladder}} = 75$	-1.01	1.90	-4.93	-0.24	8.48	-6.94	-1.13	14.94	-8.61	-9.89	22.70	-9.72	-9.27	27.66	-11.28	
		$U^{0.30}_{\text{Rectum}} = 70$	-0.83	2.20	-5.11	1.41	7.97	-6.33	4.89	14.66	-8.00	0.14	22.23	-9.34	-4.58	28.55	-10.80	
		$U^{0.10}_{\text{Rectum}} = 75$	-0.22	3.42	-3.90	1.65	9.14	-5.91	3.98	16.31	-7.73	-0.17	24.58	-9.33	-4.62	31.04	-10.70	
	0.7	$L^{0.95}_{\text{Prostate PTV}} = 75.6$	-0.49	-5.03	3.60	0.49	-9.13	8.15	4.39	-13.38	12.58	11.36	-17.89	16.82	17.71	-22.88	20.78	
		$U^{0.05}_{\text{Prostate PTV}} = 83$	-0.96	4.21	-5.22	0.08	11.16	-8.27	-0.90	19.50	-10.79	-5.30	29.06	-12.85	-9.39	40.58	-14.62	
		$U^{0.30}_{\text{Bladder}} = 70$	-16.13	-14.75	-20.18	-10.23	-6.93	-19.41	-14.47	2.06	-21.64	-17.98	8.02	-23.32	-21.12	11.49	-22.97	
		$U^{0.10}_{\text{Bladder}} = 75$	-1.90	2.43	-5.27	0.75	9.62	-7.74	-2.45	17.98	-9.43	-7.26	29.18	-12.01	-14.11	29.24	-13.08	
		$U^{0.30}_{\text{Rectum}} = 70$	-0.59	3.07	-4.86	1.33	9.20	-7.08	5.39	16.81	-9.24	0.22	25.43	-11.24	-4.66	36.38	-12.96	
		$U^{0.10}_{\text{Rectum}} = 75$	-0.02	4.28	-4.32	1.76	10.62	-6.84	4.14	19.48	-8.69	-0.76	28.61	-10.85	-5.32	38.92	-12.63	
	0.8	$L^{0.95}_{\text{Prostate PTV}} = 75.6$	-0.49	-5.72	4.18	0.70	-10.43	9.36	5.87	-15.47	14.10	12.69	-21.12	18.71	19.09	-26.48	22.91	
		$U^{0.05}_{\text{Prostate PTV}} = 83$	-0.88	4.93	-5.68	0.20	12.90	-9.24	-1.90	22.60	-11.85	-6.29	34.40	-14.08	-10.17	47.62	-16.25	
		$U^{0.30}_{\text{Bladder}} = 70$	-16.47	-11.87	-16.56	-13.29	-4.40	-19.17	-8.96	8.20	-21.96	-14.84	15.51	-21.94	-20.11	18.22	-21.91	
		$U^{0.10}_{\text{Bladder}} = 75$	-0.45	4.09	-5.56	-0.60	11.40	-9.34	-2.77	20.41	-11.28	-8.28	32.85	-14.22	-14.74	38.00	-15.79	
		$U^{0.30}_{\text{Rectum}} = 70$	-0.90	3.77	-5.21	1.23	10.57	-8.05	3.43	19.08	-10.70	-1.17	30.25	-13.37	-5.94	44.38	-14.71	
		$U^{0.10}_{\text{Rectum}} = 75$	-0.17	4.83	-5.02	1.80	12.54	-7.79	2.99	21.39	-10.00	-2.23	33.02	-13.03	-6.61	48.45	-14.76	
	0.9	$L^{0.95}_{\text{Prostate PTV}} = 75.6$	-0.36	-6.32	4.77	0.95	-11.91	10.39	7.25	-17.78	15.55	14.97	-24.86	20.53	20.76	-29.93	24.90	
		$U^{0.05}_{\text{Prostate PTV}} = 83$	-0.85	5.86	-6.06	0.43	14.98	-10.02	-3.05	26.16	-12.79	-8.03	40.43	-15.34	-11.52	54.67	-17.41	
		$U^{0.30}_{\text{Bladder}} = 70$	-19.27	-11.60	-23.79	-13.74	-2.28	-20.88	-12.12	2.69	-25.29	-25.95	19.46	-28.05	-24.02	25.30	-25.77	
		$U^{0.10}_{\text{Bladder}} = 75$	-0.90	4.64	-6.62	0.72	13.53	-9.46	-4.09	24.75	-13.10	-13.64	38.51	-16.21	-15.60	41.97	-18.61	
		$U^{0.30}_{\text{Rectum}} = 70$	-1.12	3.64	-7.03	1.13	12.35	-9.31	3.54	22.73	-11.92	-1.68	35.35	-14.08	-6.63	50.74	-16.33	
		$U^{0.10}_{\text{Rectum}} = 75$	-0.18	5.60	-5.46	1.78	14.60	-8.65	2.09	25.37	-11.54	-2.91	38.18	-14.20	-7.32	54.38	-15.98	
	1.0	$L^{0.95}_{\text{Prostate PTV}} = 75.6$	-0.30	-6.90	5.38	1.18	-13.40	11.34	8.83	-20.56	16.99	16.20	-29.64	21.88	22.74	-35.48	26.75	
		$U^{0.05}_{\text{Prostate PTV}} = 83$	-0.72	6.78	-6.64	0.63	16.96	-10.72	-4.22	30.45	-14.01	-8.82	47.28	-16.71	-13.06	64.06	-19.23	
		$U^{0.30}_{\text{Bladder}} = 70$	-16.31	-11.49	-21.18	-11.32	-2.83	-27.11	-15.25	7.84	-22.84	-17.94	19.85	-25.12	-20.80	28.96	-27.70	
		$U^{0.10}_{\text{Bladder}} = 75$	-0.92	5.23	-6.97	-0.73	15.11	-10.88	-6.00	27.99	-13.85	-9.13	40.16	-16.64	-15.08	46.74	-19.51	
		$U^{0.30}_{\text{Rectum}} = 70$	-0.23	4.82	-6.87	1.06	14.54	-10.15	1.84	23.75	-12.93	-3.39	40.02	-16.20	-9.80	58.05	-18.24	
		$U^{0.10}_{\text{Rectum}} = 75$	0.17	6.33	-5.78	1.46	15.84	-9.87	0.37	27.39	-13.31	-4.22	44.28	-15.52	-9.91	62.33	-18.50	

At the end of this subsection, we compare the computation times of SLPM and SLPM-R. Table 6 shows the entire computation time which includes the times to construct the input matrices for LP problems, to solve the successive five LP problems ($K = 5$), and to calculate the DVHs. In particular, solving LP problems occupies the most computation time (more than 90%). Note that SLPM in [12] does not use γ. For SLPM-R, the table reports the computation time for each γ.

From the results on C-Shape, we can observe that adding uncertainty into the original influence matrix dose not affect the computation times remarkably, since the computation times with $\gamma = 0.1$ and $\gamma = 1.0$ are almost same, and a strong tendency of the computation time along

Table 5: Derivations from DVCs in MultiTarget

				δ															
				0.1			0.2			0.3			0.4			0.5			
		DVCs		SLPM-R	minus	plus	SLPM-R	minus	plus	SLPM-R	minus	plus	SLPM-R	minus	plus	SLPM-R	minus	plus	
γ	0.1	$L^{0.99}_{\text{Center}}$	= 50	1.91	1.57	2.17	2.17	1.46	2.90	2.35	1.21	3.57	2.82	1.21	4.60	3.23	0.98	5.46	
		$U^{0.1}_{\text{Center}}$	= 53	1.75	2.25	1.35	2.04	3.00	1.26	2.09	3.60	0.90	2.69	4.68	0.66	3.01	5.74	0.37	
		$L^{0.99}_{\text{Superior}}$	= 25	2.04	1.66	1.90	2.55	1.77	2.23	3.13	1.85	2.69	4.14	2.33	2.86	5.04	2.97	3.41	
		$U^{0.1}_{\text{Superior}}$	= 35	1.98	1.96	1.52	2.55	2.61	1.53	2.77	3.45	1.44	3.81	4.68	1.44	4.59	5.68	1.45	
		$L^{0.99}_{\text{Inferior}}$	= 12.5	2.12	1.78	1.85	2.82	2.06	2.09	3.48	2.30	2.36	4.53	2.87	2.55	5.83	3.61	2.82	
		$U^{0.1}_{\text{Inferior}}$	= 25	2.05	1.93	1.65	2.71	2.49	1.65	2.94	2.98	1.64	4.14	4.29	1.68	5.13	5.27	1.66	
	0.2	$L^{0.99}_{\text{Center}}$	= 50	2.02	1.27	2.81	2.08	0.60	3.89	2.71	0.36	5.33	3.37	-0.18	6.31	3.96	-0.60	7.90	
		$U^{0.1}_{\text{Center}}$	= 53	1.75	2.77	1.02	2.12	4.18	0.50	2.32	5.63	-0.02	2.78	7.15	-0.72	3.62	9.12	-1.37	
		$L^{0.99}_{\text{Superior}}$	= 25	2.30	1.54	2.22	3.23	1.74	2.81	4.46	2.01	3.63	5.79	2.46	4.28	7.26	3.27	4.80	
		$U^{0.1}_{\text{Superior}}$	= 35	2.09	2.45	1.23	2.79	3.77	1.05	3.78	5.23	1.22	4.76	6.70	0.90	5.82	8.79	0.88	
		$L^{0.99}_{\text{Inferior}}$	= 12.5	2.53	1.82	2.04	3.73	2.16	2.45	5.15	2.53	3.00	6.66	3.31	3.51	8.74	4.53	3.92	
		$U^{0.1}_{\text{Inferior}}$	= 25	2.31	2.29	1.47	3.25	3.16	1.41	3.99	4.52	1.43	5.56	6.00	1.41	6.47	7.74	1.46	
	0.3	$L^{0.99}_{\text{Center}}$	= 50	2.08	0.91	3.19	2.38	0.20	4.79	2.70	-0.65	6.48	3.54	-1.79	8.31	3.95	-2.55	9.85	
		$U^{0.1}_{\text{Center}}$	= 53	1.72	3.29	0.70	2.02	5.30	-0.19	2.50	7.55	-1.09	3.22	9.73	-1.90	3.83	12.32	-2.96	
		$L^{0.99}_{\text{Superior}}$	= 25	2.61	1.42	2.49	3.64	1.34	3.43	5.81	2.00	4.48	7.70	2.37	5.16	9.51	2.53	6.22	
		$U^{0.1}_{\text{Superior}}$	= 35	2.32	2.84	1.16	3.15	4.64	0.77	4.60	7.11	0.64	5.44	9.52	0.00	7.13	11.49	0.29	
		$L^{0.99}_{\text{Inferior}}$	= 12.5	2.89	1.74	2.20	4.55	2.04	2.83	6.62	2.95	3.45	8.96	4.03	4.08	9.55	4.99	4.69	
		$U^{0.1}_{\text{Inferior}}$	= 25	2.48	2.66	1.41	3.70	3.85	1.18	5.29	5.95	1.22	6.43	8.13	0.94	7.90	10.78	0.65	
	0.4	$L^{0.99}_{\text{Center}}$	= 50	2.03	0.59	3.70	2.64	-0.45	5.62	3.32	-1.46	7.59	3.94	-3.02	9.95	4.81	-4.06	11.68	
		$U^{0.1}_{\text{Center}}$	= 53	1.85	3.84	0.32	2.16	6.39	-0.99	2.58	9.29	-2.14	3.56	12.69	-3.39	4.35	16.28	-4.56	
		$L^{0.99}_{\text{Superior}}$	= 25	2.93	1.31	2.80	4.53	1.28	3.83	6.74	1.56	5.06	9.03	2.33	5.78	10.85	1.85	7.07	
		$U^{0.1}_{\text{Superior}}$	= 35	2.46	3.29	1.23	3.47	5.75	0.47	5.06	8.05	-0.05	6.38	11.69	-0.69	6.86	14.71	-1.03	
		$L^{0.99}_{\text{Inferior}}$	= 12.5	3.34	1.82	2.34	5.42	2.27	3.02	7.72	3.24	3.74	8.39	4.48	4.43	10.22	5.39	5.18	
		$U^{0.1}_{\text{Inferior}}$	= 25	2.85	2.97	1.28	4.15	4.63	0.88	5.61	7.01	0.72	7.76	10.95	0.44	8.87	13.09	0.34	
	0.5	$L^{0.99}_{\text{Center}}$	= 50	2.07	0.20	4.02	2.67	-1.16	6.37	3.37	-2.98	8.43	3.91	-4.63	11.09	5.40	-6.48	12.96	
		$U^{0.1}_{\text{Center}}$	= 53	1.84	4.34	-0.07	2.28	7.54	-1.36	2.71	11.00	-3.08	3.71	15.33	-4.41	4.71	20.58	-5.64	
		$L^{0.99}_{\text{Superior}}$	= 25	3.12	1.22	2.96	5.08	1.01	4.19	7.16	1.07	5.32	10.87	1.53	6.63	12.85	3.10	8.31	
		$U^{0.1}_{\text{Superior}}$	= 35	2.60	3.53	0.75	3.54	6.35	-0.12	4.54	9.67	-0.58	6.68	13.46	-1.28	7.47	17.63	-2.13	
		$L^{0.99}_{\text{Inferior}}$	= 12.5	3.66	1.72	2.39	6.17	2.20	3.27	9.01	2.92	4.06	9.38	4.57	4.92	9.34	5.50	5.76	
		$U^{0.1}_{\text{Inferior}}$	= 25	2.86	3.23	1.02	4.37	5.41	0.61	6.18	7.68	0.42	8.40	11.96	-0.32	10.31	16.12	-0.08	
	0.6	$L^{0.99}_{\text{Center}}$	= 50	2.27	-0.12	4.52	2.67	-2.20	7.05	3.55	-4.34	9.79	4.74	-6.46	12.35	5.97	-8.92	15.24	
		$U^{0.1}_{\text{Center}}$	= 53	1.71	4.94	-0.45	1.97	8.59	-2.33	2.76	13.00	-4.00	3.80	18.54	-5.70	5.29	25.14	-6.82	
		$L^{0.99}_{\text{Superior}}$	= 25	3.39	0.92	3.10	5.66	0.54	4.61	9.05	1.15	5.97	12.31	1.15	7.44	16.43	2.91	8.85	
		$U^{0.1}_{\text{Superior}}$	= 35	2.67	3.96	0.42	3.99	6.98	-0.65	5.83	11.39	-1.37	6.94	14.89	-2.28	9.02	22.93	-2.84	
		$L^{0.99}_{\text{Inferior}}$	= 12.5	4.02	1.61	2.54	6.98	1.95	3.41	9.35	3.36	4.41	8.91	4.79	5.08	9.39	7.43	6.08	
		$U^{0.1}_{\text{Inferior}}$	= 25	2.99	3.41	0.90	4.96	5.96	0.34	6.67	9.79	-0.33	8.78	13.93	-0.83	11.09	19.86	-1.17	
	0.7	$L^{0.99}_{\text{Center}}$	= 50	2.26	-0.53	4.82	2.82	-3.05	8.03	3.98	-5.17	10.97	5.14	-8.47	13.65	6.49	-11.19	16.26	
		$U^{0.1}_{\text{Center}}$	= 53	1.70	5.48	-0.83	1.95	9.68	-3.02	2.76	14.96	-4.96	4.04	21.68	-6.69	5.34	29.86	-7.95	
		$L^{0.99}_{\text{Superior}}$	= 25	3.70	0.92	3.36	6.12	0.23	4.89	9.87	0.70	6.64	14.14	0.89	7.95	18.83	1.78	9.50	
		$U^{0.1}_{\text{Superior}}$	= 35	2.92	4.59	0.16	3.77	8.03	-1.09	5.94	13.24	-2.27	7.41	19.47	-3.19	9.09	25.00	-3.60	
		$L^{0.99}_{\text{Inferior}}$	= 12.5	4.39	1.62	2.66	7.58	1.85	3.55	10.22	3.17	4.58	9.44	5.01	5.53	9.07	7.67	6.36	
		$U^{0.1}_{\text{Inferior}}$	= 25	3.32	3.81	0.76	5.05	6.55	-0.08	7.03	11.12	-0.72	9.11	16.64	-1.01	11.41	22.35	-1.95	
	0.8	$L^{0.99}_{\text{Center}}$	= 50	2.23	-0.94	5.23	2.77	-3.82	8.50	4.22	-6.58	11.79	5.13	-10.68	14.54	6.94	-14.41	17.71	
		$U^{0.1}_{\text{Center}}$	= 53	1.76	6.03	-1.20	2.02	11.20	-3.66	2.96	17.33	-5.73	4.22	25.59	-7.46	6.03	36.50	-9.23	
		$L^{0.99}_{\text{Superior}}$	= 25	3.89	0.71	3.52	6.79	-0.26	5.16	10.95	0.18	6.81	15.88	0.54	8.55	19.28	0.67	10.21	
		$U^{0.1}_{\text{Superior}}$	= 35	2.83	4.81	-0.01	4.31	9.03	-1.36	5.83	14.51	-2.93	7.44	21.22	-3.94	9.54	30.53	-4.98	
		$L^{0.99}_{\text{Inferior}}$	= 12.5	4.73	1.55	2.73	8.48	1.87	3.77	9.15	3.06	4.75	8.99	4.74	5.69	9.22	5.66	6.49	
		$U^{0.1}_{\text{Inferior}}$	= 25	3.45	4.05	0.50	5.36	7.11	-0.50	7.43	12.38	-1.29	9.80	18.79	-2.11	12.30	26.83	-2.35	
	0.9	$L^{0.99}_{\text{Center}}$	= 50	2.26	-1.28	5.74	3.17	-4.51	9.36	4.56	-8.01	12.95	5.65	-12.72	15.74	7.68	-18.19	19.20	
		$U^{0.1}_{\text{Center}}$	= 53	1.64	6.50	-1.58	2.18	12.37	-4.21	3.16	19.64	-6.65	4.32	29.00	-8.43	5.67	42.54	-10.36	
		$L^{0.99}_{\text{Superior}}$	= 25	3.98	0.32	3.65	7.41	-0.44	5.63	11.99	-0.50	7.43	17.17	-1.56	8.95	22.25	-2.58	10.56	
		$U^{0.1}_{\text{Superior}}$	= 35	2.90	5.10	-0.36	4.60	9.83	-1.89	6.01	16.43	-3.43	7.56	23.70	-4.58	9.01	35.12	-6.01	
		$L^{0.99}_{\text{Inferior}}$	= 12.5	5.03	1.42	2.83	9.40	1.69	3.87	9.26	2.82	4.83	8.94	4.55	5.75	9.36	5.16	6.73	
		$U^{0.1}_{\text{Inferior}}$	= 25	3.63	4.29	0.33	5.70	8.11	-0.82	8.05	13.98	-1.62	10.14	21.19	-2.50	12.42	30.24	-3.28	
	1.0	$L^{0.99}_{\text{Center}}$	= 50	2.46	-1.55	6.22	3.35	-5.24	10.10	4.51	-9.72	13.83	6.37	-15.01	17.16	8.03	-22.28	20.25	
		$U^{0.1}_{\text{Center}}$	= 53	1.57	6.99	-1.94	2.11	13.61	-4.88	3.02	22.08	-7.48	4.53	33.65	-9.39	5.49	48.52	-11.34	
		$L^{0.99}_{\text{Superior}}$	= 25	4.27	0.28	3.93	8.03	-0.80	5.80	12.90	-1.71	7.56	19.06	-1.58	9.42	21.82	-2.04	10.84	
		$U^{0.1}_{\text{Superior}}$	= 35	2.84	5.54	-0.63	4.55	10.77	-2.49	6.23	17.82	-4.20	7.41	27.75	-5.38	9.45	39.98	-6.84	
		$L^{0.99}_{\text{Inferior}}$	= 12.5	5.38	1.39	2.86	10.25	1.56	4.05	9.92	2.60	5.01	9.08	4.64	5.89	9.05	3.91	6.59	
		$U^{0.1}_{\text{Inferior}}$	= 25	3.69	4.59	0.17	5.97	8.55	-1.25	7.91	14.45	-2.20	9.93	22.49	-3.37	12.90	34.61	-3.81	

with the increment in γ cannot be seen. The numbers of variables in the first LP problems in SLPM and SLPM-R are 38549 and 76680, respectively. The difference of 38131 corresponds to $\sum_{s\in\mathcal{S}}\left\{|\mathcal{I}_s|\times(|\underline{A}_s|+|\overline{A}_s|)\right\}$ due to the split of variables z_{si} into $\underline{z}_{si}$ and $\overline{z}_{si}$ in deriving the robust counterpart (8). Therefore, the number of variables is almost twice in SLPM-R, but Table 2 implies the increment in the computation time is only about $\frac{170-125}{125}\sim 36\%$.

We can see similar tendencies in the Prostate and MultiTarget data. However, in the Head and Neck data, SLPM-R is faster than SLPM. Since the Head and Neck dataset involves the largest

Table 6: The entire computation time for different γ (time in seconds)

	SLPM	SLPM-R									
γ	–	0.1	0.2	0.3	0.4	0.5	0.6	0.7	0.8	0.9	1.0
C-Shape	125.2	167.1	163.8	161.1	162.7	164.8	165.7	164.2	169.2	169.7	173.0
Head and Neck	1893.1	1638.1	1424.1	1448.2	1420.5	1382.3	1320.4	1383.5	1367.2	1456.9	1444.5
Prostate	266.0	503.3	500.7	472.6	376.5	406.0	403.4	387.9	380.9	347.5	366.7
MultiTarget	365.5	754.4	809.3	828.8	816.0	792.6	808.2	821.6	671.2	706.2	811.3

number of voxels and SLPM solves the worst cases, the large deviations from D_s^0 might affect the convergence of the interior-point method implemented in CPLEX.

4.2 Numerical Results with Penalty Terms

In Table 7, we compare the deviations from DVCs in the results of the simple objective function t in (8a) and those of the objective function with the penalty term (10) introduced in Section 3.3. Here, we fix the parameters at $(\gamma, \delta) = (0.5, 0.2)$. We use the thresholds of DVCs for the parameters θ in (10), more precisely, $\underline{\theta}_s^\alpha = L_s^\alpha$, $\overline{\theta}_s^\alpha = U_s^\alpha$, $\underline{\theta}_s = L_s$, and $\overline{\theta}_s = U_s$, and we set the penalty weight λ in (10) as Table 7. We should use large λ to give a high penalty for the deviations from DVCs, but, if λ is set too large, the relative importance of minimizing t in the objective function becomes small, thus the effect of hot and cold spots will also be decreased. To examine the effectiveness of the penalty terms, we chose λ based on preliminary experiments.

We first focus the results of Head and Neck. When we use the simple objective function (8a), the two worst cases of SLPM and even SLPM-R cannot satisfy all the DVCs. On the contrary, if we use the penalty term (10), SLPM-R can output the solution that fulfills all the DVCs. In particular, the penalty terms are effective to reduce the deviations from $U^{0.5}_{\text{Lt Parotid}}$ and $U^{0.5}_{\text{Rt Parotid}}$.

As for C-Shape, the parameters λ of Outer Target and Core were set to 0.4 and 0.1, respectively, in order to prioritize Outer Target, since the constraints of Outer Target are severe. SLPM-R with the penalty terms finds a solution satisfying both DVCs for PTV (Outer Target) as desired, on the other hand, the deviation from the DVC on Core is worse.

In the Prostate dataset, we also set higher values $\lambda = 0.6$ for Prostate PTV to give a higher priority. Though the deviation at one DVC ($U^{0.10}_{\text{Rectum}}$) still remains, all of the other DVCs are fulfilled.

In the MultiTarget dataset, it was difficult to find a solution satisfying all DVCs as shown in Section 4.1. The three structures are PTVs in this dataset, and we should give a higher priority to a structure with high threshold, since the change in high-dose areas can be considered more important, thus we set large parameters λ to the DVCs of Center. In accordance with such parameters setting, SLPM-R with the penalty terms can reduce the deviations from DVCs on Center.

Compared to the worst cases by the existing method (SLPM), the proposed method reflects the parameters. For example, in the Prostate dataset, we set higher λ to PTV, thus the proposed method can satisfy the two DVCs on PTV, while the worse cases of SLPM can satisfy only one of the two DVCs. Similar results can be found in C-Shape and Head and Neck results.

5 Discussion

Since one of advantages of IMRT is the capability of giving more flexibility to the control of beamlets, it is expected that IMRT can improve plans for structures with movements like lungs. Here, we discuss an extension of our approach to the variations by breathing.

Table 7: Numerical results with penalty terms for $(\gamma, \delta) = (0.5, 0.2)$

C-Shape									
				without penalty (8a)			with penalty (10)		
DVC			λ	SLPM-R	minus	plus	SLPM-R	minus	plus
$L^{0.95}_{\text{Outer Target}}$	=	50	0.4	0.52	-3.91	4.41	-0.05	-3.95	4.40
$U^{0.1}_{\text{Outer Target}}$	=	55	0.4	0.44	5.65	-3.80	-0.06	5.56	-3.86
$U^{0.1}_{\text{Core}}$	=	25	0.1	3.15	3.58	-1.09	12.73	6.09	0.23
Head and Neck									
				without penalty (8a)			with penalty (10)		
DVC			λ	SLPM-R	minus	plus	SLPM-R	minus	plus
$L^{0.9}_{\text{PTV}}$	=	50	0.2	-0.34	-4.88	3.27	-0.32	-0.48	3.28
$L^{0.99}_{\text{PTV}}$	=	46.5	0.2	-0.87	-5.23	2.85	-0.43	-5.11	2.88
$U^{0.2}_{\text{PTV}}$	=	55	0.2	-0.44	4.33	-4.64	-0.32	4.33	-4.57
U_{Cord}	=	40	0.1	-2.14	5.29	-2.42	-0.77	5.09	-1.90
$U^{0.5}_{\text{Lt Parotid}}$	=	20	0.1	1.72	0.51	-2.50	-2.30	1.14	-2.73
$U^{0.5}_{\text{Rt Parotid}}$	=	20	0.1	1.45	0.85	-2.54	-1.38	1.45	-2.96
Prostate									
				without penalty (8a)			with penalty (10)		
DVC			λ	SLPM-R	minus	plus	SLPM-R	minus	plus
$L^{0.95}_{\text{Prostate PTV}}$	=	75.6	0.6	0.06	-6.63	5.96	-0.05	-6.88	5.87
$U^{0.05}_{\text{Prostate PTV}}$	=	83	0.6	-0.41	7.34	-6.54	-0.42	7.42	-6.74
$U^{0.30}_{\text{Bladder}}$	=	70	0.1	-12.44	-11.54	-16.32	-23.39	-16.643	-22.01
$U^{0.10}_{\text{Bladder}}$	=	75	0.1	-0.21	6.94	-5.90	-9.00	1.42	-8.45
$U^{0.30}_{\text{Rectum}}$	=	70	0.2	0.47	6.30	-0.68	-0.78	6.56	-5.58
$U^{0.10}_{\text{Rectum}}$	=	75	0.2	1.15	7.42	-5.22	2.63	8.47	-4.48
MultiTarget									
				without penalty (8a)			with penalty (10)		
DVC			λ	SLPM-R	minus	plus	SLPM-R	minus	plus
$L^{0.99}_{\text{Center}}$	=	50	1.0	2.67	-1.16	6.37	1.48	-2.26	5.86
$U^{0.1}_{\text{Center}}$	=	53	1.0	2.28	7.54	-1.36	1.11	6.75	-2.33
$L^{0.99}_{\text{Superior}}$	=	25	0.2	5.08	1.01	4.19	0.09	0.45	5.17
$U^{0.1}_{\text{Superior}}$	=	35	0.2	3.54	6.35	-0.12	11.26	11.61	3.23
$L^{0.99}_{\text{Inferior}}$	=	12.5	0.1	6.17	2.20	3.27	2.43	5.41	6.43
$U^{0.1}_{\text{Inferior}}$	=	25	0.1	4.37	5.41	0.61	16.35	10.56	3.90

Chan et al. [4, 5] proposed an iterative algorithm to compute beamlet intensities reflecting a lung state at each iteration based on an assumption that the lung state transitions periodically due to breathing, but with some uncertainty. Let $\mathcal{X}$ be a finite set of lung states and $\mathcal{P}$ be a set of probability mass functions (PMFs):

$$\mathcal{P} = \{p \in \mathbb{R}^{|\mathcal{X}|} : \sum_{\chi \in \mathcal{X}} p(\chi) = 1, \quad p(\chi) \geq 0 \ \forall \chi \in \mathcal{X}\}.$$

In other words, $p(\chi)$ is the probability that the lung takes a state $\chi \in \mathcal{X}$.

Let $\tilde{p} \in \mathcal{P}$ be a nominal PMF in $\mathcal{P}$. The set of lung states $\mathcal{X}$ can be divided into two sets $\mathcal{U}(\subset \mathcal{X})$ and $\mathcal{X}\backslash\mathcal{U}$, where $\mathcal{U}$ specifies locations that the realized PMF is allowed to deviate from the nominal one $\tilde{p}$. Chan et al. considered the following uncertainty set:

$$\tilde{\mathcal{P}} = \left\{p \in \mathcal{P} : \tilde{p}(\chi) - \underline{p}(\chi) \leq p(\chi) \leq \tilde{p}(\chi) + \overline{p}(\chi) \ \forall \chi \in \mathcal{U}, \quad p(\chi) = \tilde{p}(\chi) \ \forall \chi \in \mathcal{X}\backslash\mathcal{U}\right\},$$

where $\underline{p}$ and $\overline{p}$ determines the interval in $\mathcal{P}$, and they computed the absorbed dose of voxel $i \in \mathcal{I}_s$ of an organ s as $\sum_{\chi \in \mathcal{X}} \sum_{j \in \mathcal{J}} (\Delta_{\chi,s})_{ij} \tilde{p}(\chi) x_j$, where $(\Delta_{\chi,s})_{ij}$ is the (i,j)th element of influence matrix $\Delta_{\chi,s}$ for a state $\chi \in \mathcal{X}$.

We can extend the robust optimization model with the hot and cold spots (8) utilizing the uncertainty of $\tilde{\mathcal{P}}$. In (8), we considered D'_s as a perturbation to the influence matrix D_s. In a

similar way, we can introduce $\Delta'_{\chi,s}$ as a perturbation to $\Delta_{\chi,s}$. By noting this, (8) can be extended into the following bi-level optimization problem.

$$
\begin{aligned}
\min \quad & t && && (11)\\
\text{s.t.} \quad & \sum_{\chi\in\mathcal{X}}\sum_{j\in\mathcal{J}} \left\{(\Delta_{\chi,s})_{ij} - \delta|(\Delta'_{\chi,s})_{ij}|\right\}\tilde{p}(\chi)x_j = \underline{z}_{si} && s\in\mathcal{S}; i\in\mathcal{I}_s\\
& \sum_{\chi\in\mathcal{X}}\sum_{j\in\mathcal{J}} \left\{(\Delta_{\chi,s})_{ij} + \delta|(\Delta'_{\chi,s})_{ij}|\right\}\tilde{p}(\chi)x_j = \overline{z}_{si} && s\in\mathcal{S}; i\in\mathcal{I}_s\\
& L_s - \underline{P}_s t \le \underline{z}_{si} + \underline{\beta}_{si} && s\in\mathcal{S}; i\in\mathcal{I}_s\\
& \overline{z}_{si} + \overline{\beta}_{si} \le U_s + \overline{P}_s t && s\in\mathcal{S}; i\in\mathcal{I}_s\\
& \underline{\zeta}^{\alpha}_s - \frac{1}{(1-\alpha)|\mathcal{I}_s| - |\underline{R}^{\alpha}_{k,s}|}\sum_{i\in\mathcal{I}_s\setminus\underline{R}^{\alpha}_{k,s}} (\underline{\zeta}^{\alpha}_s - \underline{z}_{si})^+ \ge L^{\alpha}_s - \underline{P}^{\alpha}_s t && s\in\mathcal{S}; \alpha\in\underline{A}_s\\
& \overline{\zeta}^{\alpha}_s + \frac{1}{\alpha|\mathcal{I}_s| - |\overline{R}^{\alpha}_{k,s}|}\sum_{i\in\mathcal{I}_s\setminus\overline{R}^{\alpha}_{k,s}} (\overline{z}_{si} - \overline{\zeta}^{\alpha}_s)^+ \le U^{\alpha}_s + \overline{P}^{\alpha}_s t && s\in\mathcal{S}; \alpha\in\overline{A}_s\\
& x_j \ge 0 && j\in\mathcal{J}\\
& \underline{z}_{si},\ \overline{z}_{si} \ge 0 && s\in\mathcal{S}; i\in\mathcal{I}_s\\
& \underline{\zeta}^{\alpha}_s,\ \overline{\zeta}^{\alpha}_s,\ t : \text{free variables.}
\end{aligned}
$$

where

$$
\begin{aligned}
\underline{\beta}_{si} = \min_{p} \quad & \sum_{\chi\in\mathcal{U}}\sum_{j\in\mathcal{J}} \left\{(\Delta_{\chi,s})_{ij} + \delta|(\Delta'_{\chi,s})_{ij}|\right\}(p(\chi) - \tilde{p}(\chi))x_j && (12)\\
\text{s.t.} \quad & p\in\tilde{\mathcal{P}}
\end{aligned}
$$

and

$$
\begin{aligned}
\overline{\beta}_{si} = \max_{p} \quad & \sum_{\chi\in\mathcal{U}}\sum_{j\in\mathcal{J}} \left\{(\Delta_{\chi,s})_{ij} + \delta|(\Delta'_{\chi,s})_{ij}|\right\}(p(\chi) - \tilde{p}(\chi))x_j && (13)\\
\text{s.t.} \quad & p\in\tilde{\mathcal{P}}.
\end{aligned}
$$

Here, $\underline{\beta}_{si}$ is the largest negative possible change caused by $p\in\tilde{\mathcal{P}}$. Similarly, $\overline{\beta}_{si}$ is the largest positive possible change.

The extended problem (11) is not a standard LP problem, since $\underline{\beta}_{si}$ and $\overline{\beta}_{si}$ are determined by the lower-level LP problems (12) and (13). However, by following a procedure discussed in Bortfeld et al. [2] that exploits the duality theorem on LP, we can reformulate (11) as a standard LP problem, therefore, (11) can be substantially solved with interior-point methods.

This approach can consider not only uncertainty contained in the influence matrix but also uncertainty contained in the probability of states at the same time. Though this approach requires more variables than the proposed method and a longer computation time, it would derive more practical treatment plans.

6 Conclusions and Future Directions

In this paper, we extended SLPM with a framework of robust optimization. We mathematically showed that the proposed method holds the three favorable properties of SLPM. In particular, when the objective function in the LP problem is non-positive, the proposed method SLPM-R can satisfy all the DVCs even when it takes the uncertainty in the influence matrix into consideration.

Through the numerical experiments, we observed that SLPM-R provides a solution that reduces the deviation from DVCs compared to SLPM and this can lead to a more suitable treatment plan. In contrast, SLPM-R requires more computation time than SLPM due to the increased number of variables in LP problems. By introducing the penalty terms in the objective function, we can give priorities to DVCs and SLPM-R can find a solution that fulfills all the DVCs for the Head and Neck dataset.

Regarding future work, there are mainly two directions, to develop more practical models and to improve the computation time. With respect to the former, the proposed method can be applied to lungs or plural influence matrices by assuming that each state transitions stochastically, as discussed in Section 5. Furthermore, Chan et al. [5] developed an algorithm for dividing irradiations into small amounts with several steps so that the irradiations can be adjusted in latter steps. We may combine this idea with the proposed method.

In regard to the computation time, one way is to accelerate an interior-point method by using the structure when formulating FMO as LP problems in a similar way to Enberg et al. [9]. In particular, it may be possible to utilize the structure defined by the additional variables ζ and z. Arc-search type interior-point methods [19, 20] can also be discussed.

References

[1] A. Ben-Tal, L. El Ghaoui, and A. Nemirovski. *Robust optimization*. Princeton University Press, 2009.

[2] T. Bortfeld, T. C. Chan, A. Trofimov, and J. N. Tsitsiklis. Robust management of motion uncertainty in intensity-modulated radiation therapy. *Operations Research*, 56(6):1461–1473, 2008.

[3] Cancer Research UK. Intensity modulated radiotherapy (IMRT). `https://www.cancerresearchuk.org/about-cancer/cancer-in-general/treatment/radiotherapy/external/types/intensity-modulated-radiotherapy-imrt`. Accessed November 8, 2021.

[4] T. C. Chan, T. Bortfeld, and J. N. Tsitsiklis. A robust approach to imrt optimization. *Physics in Medicine & Biology*, 51(10):2567, 2006.

[5] T. C. Chan and V. V. Mišić. Adaptive and robust radiation therapy optimization for lung cancer. *European Journal of Operational Research*, 231(3):745–756, 2013.

[6] V. Chvatal. *Linear programming*. Macmillan, 1983.

[7] J. O. Deasy, A. I. Blanco, and V. H. Clark. CERR: a computational environment for radiotherapy research. *Medical Physics*, 30(5):979–985, 2003.

[8] J. Dias, H. Rocha, B. Ferreira, and M. do Carmo Lopes. A genetic algorithm with neural network fitness function evaluation for IMRT beam angle optimization. *Central European Journal of Operations Research*, 22(3):431–455, 2014.

[9] L. Engberg, A. Forsgren, K. Eriksson, and B. Hårdemark. Explicit optimization of plan quality measures in intensity-modulated radiation therapy treatment planning. *Medical Physics*, 44(6):2045–2053, 2017.

[10] G. A. Ezzell, J. W. Burmeister, N. Dogan, T. J. LoSasso, J. G. Mechalakos, D. Mihailidis, A. Molineu, J. R. Palta, C. R. Ramsey, B. J. Salter, et al. IMRT commissioning: multiple institution planning and dosimetry comparisons, a report from AAPM Task Group 119. *Medical Physics*, 36(11):5359–5373, 2009.

[11] E. Kalinin and J. Deasy. A method for fast 3-D IMRT dose calculations: The quadrant infinite beam (QIB) algorithm. *Medical Physics*, 30(6):1348–1349, 2003.

[12] S. Kishimoto and M. Yamashita. A successive LP approach with C-VaR type constraints for IMRT optimization. *Operations Research for Health Care*, 17:55–64, 2018.

[13] R. T. Rockafellar and S. Uryasev. Optimization of conditional value-at-risk. *Journal of Risk*, 2:21–42, 2000.

[14] H. E. Romeijn, R. K. Ahuja, J. F. Dempsey, and A. Kumar. A new linear programming approach to radiation therapy treatment planning problems. *Operations Research*, 54(2):201–216, 2006.

[15] H. E. Romeijn, R. K. Ahuja, J. F. Dempsey, A. Kumar, and J. G. Li. A novel linear programming approach to fluence map optimization for intensity modulated radiation therapy treatment planning. *Physics in Medicine & Biology*, 48(21):3521, 2003.

[16] A. L. Soyster. Convex programming with set-inclusive constraints and applications to inexact linear programming. *Operations research*, 21(5):1154–1157, 1973.

[17] B. Stemkens, R. H. Tijssen, B. D. De Senneville, J. J. Lagendijk, and C. A. Van Den Berg. Image-driven, model-based 3d abdominal motion estimation for mr-guided radiotherapy. *Physics in Medicine & Biology*, 61(14):5335, 2016.

[18] A. T. Tuncel, F. Preciado, R. L. Rardin, M. Langer, and J.-P. P. Richard. Strong valid inequalities for fluence map optimization problem under dose-volume restrictions. *Annals of Operations Research*, 196(1):819–840, 2012.

[19] M. Yamashita, E. Iida, and Y. Yang. An infeasible interior-point arc-search algorithm for nonlinear constrained optimization. *Numerical Algorithms*, 2021. to appear.

[20] Y. Yang and M. Yamashita. An arc-search $O(nL)$ infeasible-interior-point algorithm for linear programming. *Optimization Letters*, 12(4):781–798, 2018.